Heliyon 10 (2024) e28963

Contents lists available at ScienceDirect

Heliyon

journal homepage: www.cell.com/heliyon

Research article

T-spherical fuzzy interactive Dubois–Prade information aggregation approach for evaluating low-carbon technology impact and environmental mitigation

Toqeer Jameel [a], Muhammad Riaz [a], Naveed Yaqoob [b,*], Muhammad Aslam [c]

[a] Department of Mathematics, University of the Punjab, Lahore, Pakistan
[b] Department of Mathematics and Statistics, Riphah International University, I-14 Islamabad 46000, Pakistan
[c] Department of Mathematics, College of Sciences, King Khalid University, Abha 61413, Saudi Arabia

ARTICLE INFO

Keywords:
T-spherical fuzzy numbers
Dubois–Prade operations
Aggregation operators
Power system reforms
Low-carbon technology

ABSTRACT

The concept of T-spherical fuzzy sets (T-SFSs) provides a robust optimization approach to deal with uncertainties in environmental concerns. The main objective of this paper is to introduce a hybrid approach for the power system reforms and advances of low-carbon technology to address environmental concerns as well as transition towards a more sustainable energy infrastructure. To meet these objectives, various aggregation operators (AOs) are developed named as T-spherical fuzzy Dubois–Prade (T-SFDP), T-spherical fuzzy interactive Dubois–Prade weighted average (T-SFIDPWA), T-spherical fuzzy interactive Dubois–Prade ordered weighted average (T-SFIDPOWA), T-spherical fuzzy interactive Dubois–Prade weighted geometric (T-SFIDPWG), and T-spherical fuzzy interactive Dubois–Prade ordered weighted geometric (T-SFIDPOWG). These AOs are integrated in the construction CRITIC-EDAS framework, facilitating a comprehensive assessment and ranking of proposals. This paper underscores the methodology's efficacy and precision through rigorous validation with CRITIC-MAUT, CRITIC-ARAS, CRITIC-EDAS, and CRITIC-MABAC analyses, showcasing its ability to discern and prioritize reform initiatives with exactitude. Beyond enhancing the comprehension of reform proposals, this hybrid approach establishes a benchmark for future evaluations, significantly contributing to the dynamic landscape of power system optimization. The methodology's clarity and precision offer decision-makers a valuable tool for the thorough assessment and prioritization of power system reforms initiatives, fostering sustainability and environmentally conscious advancements.

1. Introduction

Extreme weather occurrences and natural calamities have become increasingly intertwined with the global phenomenon of climate change since the early 2000s. The scientific consensus on human-induced climate change has prompted nations worldwide to acknowledge the urgent need for collective action. In response to this, international agreements on carbon emission reduction and neutrality objectives have emerged as a focal point for global cooperation, emphasizing the imperative of transitioning from

* Corresponding author.
E-mail addresses: toqeerjameel5656@gmail.com (T. Jameel), mriaz.math@pu.edu.pk (M. Riaz), naveed.yaqoob@riphah.edu.pk (N. Yaqoob), muamin@kku.edu.sa (M. Aslam).

https://doi.org/10.1016/j.heliyon.2024.e28963
Received 27 November 2023; Received in revised form 17 March 2024; Accepted 27 March 2024

Available online 2 April 2024

conventional energy sources to sustainable and renewable alternatives. China, as the world's foremost energy consumer and carbon emitter, plays a pivotal role in the global effort to combat climate change, with a particular focus on the electricity sector [1]. Projections from the International Energy Agency (IEA) indicate that by 2030, China's electrical sector could account for a staggering 60% of the world's coal demand, potentially surpassing the established emissions limits for the entire global electricity sector [2]. Recognizing the gravity of the situation, China has committed to implementing decisive measures to achieve a peak in carbon emissions by 2030 and attain carbon neutrality by 2060, often referred to as the ambitious "double carbon" targets [3]. Of notable concern is the significant role played by coal in China's overall emissions profile, contributing to approximately 80% of the nation's total emissions, with half of that being attributed to coal power [1,2]. As such, addressing the challenges posed by coal becomes a central theme in achieving China's ambitious carbon reduction goals. Consequently, the power industry emerges as a critical arena for efforts to reduce carbon emissions and reshape the trajectory of China's contemporary energy landscape. The ongoing process of electrification within society marks a significant transition, bringing with it a palpable shift in the burden of carbon reduction from terminal energy to the power industry. This transition intensifies the focus on carbon reduction within the sector, necessitating concerted efforts to enhance carbon reduction intensity. As the power sector undergoes changes and system modifications, it serves as a catalyst for increased research and development in low-carbon technology and the accelerated adoption of renewable energy sources [4]. This transformative process not only aligns with global environmental goals but also contributes substantially to the development of clean, low-carbon, safe, and efficient energy systems. Given the magnitude of the challenge and the dynamic nature of the energy sector, the development of a new energy system centered on energy efficiency becomes imperative. The quest for sustainability requires careful evaluation of ideas and strategies for system upgrades, taking into account a myriad of factors, including cost implications, system performance metrics, and expected overall effects on the environment and society. This evaluative process presents a formidable MCDM challenge [5], particularly when uncertainties surround the characteristics of the evaluation object. In such cases, the use of fuzzy concepts becomes essential for providing a comprehensive description, reminiscent of the nuanced evaluation of residents' happiness within certain contexts [6]. As we delve deeper into the subsequent sections of this paper, our exploration will focus on unraveling the intricacies of the power industry. We will systematically examine the challenges and opportunities inherent in this sector as it navigates the path toward meeting China's ambitious "double carbon" targets. The ensuing discussion will hone in on the crucial role of MCDM methodologies, with a specific emphasis on those incorporating fuzzy logic. Such methodologies become indispensable tools in navigating the complexities of decision-making within this critical domain, ensuring that strategic choices align with environmental goals and contribute to the broader mission of sustainable development [7]. Moreover, applications of decision-making can be seen in forecasting of Alzheimer's disease [8], logistics center location [9], cold chain logistics service providers [10], risk management [11], military decision-making [12] and industrial control system [13].

1.1. Literature review

In real-world scenarios, as a system grows in complexity, the task of discerning the optimal choice from a range of feasible options becomes progressively challenging for decision-makers (DMs). The difficulty of attaining a singular goal is a substantial challenge, yet it is not insurmountable. Numerous businesses have encountered the intricacies of motivating their workforce, defining objectives, and shaping perspectives. As a result, organizational decisions, whether originating from individuals or committees, encompass multiple simultaneous objectives. By employing criteria that allow for optional resolutions, each DM is constrained to formulate the most suitable solution for each practical implication in real-world issues. Consequently, DMs are increasingly dedicated to developing methods that are both more pragmatic and dependable to pinpoint the most favorable options.

Zadeh [14] pioneered the concept of "fuzzy set" (FS) as a mathematical framework to describe imprecision to navigate the complexities inherent in decision-making scenarios. This ground-breaking concept provided a way to represent uncertain and ambiguous information in decision-making processes. Atanasov [15] improved the idea by presenting "intuitionistic fuzzy sets" (IFS) as a distinct project, building on this foundation. The IFS framework considers non-membership functionality as well as membership functionalities to better address complicated decision-making circumstances. Senapati and Yager [16,17] introduced Fermatean fuzzy sets and extended the framework to weighted averaging/geometric operators, providing a flexible approach for representing uncertainty in ambient intelligence and decision-making contexts.

Alcantud [18] proposed a novel intuitionistic fuzzy aggregation approach based on weighted geometric means for multi-attribute group decision-making. Alcantud et al. [19] explored the integration of N-soft sets and rough sets, bridging two established theories and demonstrating their compatibility for handling imprecise information. Despite the efficiency of IFSs in handling several complex problems, certain scenarios continue to present hurdles that they are unable to tackle properly. This constraint is obvious when dealing with voting circumstances, as human perspectives frequently include responses like "yes," "no," "don't know," and "refuse". Traditional FS and IFS models have difficulty correctly expressing these different reactions. In response to these issues, Cuong [20] suggested the novel notion of "picture fuzzy set" (PFS) as a solution. This unique framework tries to overcome the constraints of FS and IFS models by adding visual representations, allowing for a more comprehensive and accurate picture of the human perspective in decision-making processes.

Cuong and Hai [21] developed the fundamental principles of PFSs in their research. Cuong [22] developed a method for measuring the distance between PFSs as well as a complete examination of several PFS properties. Riaz et al. [23] significantly revised core PFS operations, improving the understanding and usefulness of these sets. Phong et al. [24] investigated several PF-relation arrangements, bringing important insights into this field of inquiry. These works have substantially increased our understanding and approaches to dealing with PFSs.

There is a significant emphasis in the modern era on synthesizing knowledge and improving aggregate operators (AOs). Understanding the efficacy and limitations of AOs has become critical in decision-making. AOs provide fundamental concepts for combining a limited collection of inaccurate values into a cohesive and all-encompassing fuzzy value. Data analysis is important in many fields, including selection, business, medicine, architecture, and surveillance. Various established AOs operate on PFSs within different domains, each with particular functions and operational regulations. Garg [25] has advocated for the use of several averaging AOs for picture fuzzy numbers (PFNs). Wang et al. [26] researched the selection of a PFS-based hotel energy performance conversion project. These efforts help to advance our understanding and application of AOs in dealing with imprecise values in a variety of fields. Furthermore, Wang et al. [27] defined "Muirhead mean AOs" for picture fuzzy numbers (PFNs). To summarize, the research conducted by these varied writers has considerably advanced the subject of AOs by bringing innovative concepts, changing established approaches, and suggesting novel methodologies. These contributions lay a solid platform for future research and growth in this field.

In practical scenarios, PFS may prove inadequate, particularly when faced with situations where the combined values of PMD, N_uMD, and N_gMD exceed 1. PFS may fail to yield a meaningful conclusion under such circumstances. The limitations of PFS prompted the introduction of "spherical fuzzy sets" (SFSs) by different authors independently [28–30]. Mahmood et al. expanded upon this concept, introducing SPFSs in [30]. T-SPFSs demonstrate superior handling of uncertainty, as the sum of the t-*th* power of membership grades approaches a unit interval, outperforming traditional fuzzy structures. Munir et al. further advanced the utility of T-SPFSs by introducing Einstein hybrid AOs in [31], particularly focusing on their applications in Multi-Criteria Decision Making (MCDM). Building on this work, Zeng et al. defined Einstein interactive AOs for T-SPFSs in [32], demonstrating their application in the selection of photovoltaic cells. This body of research signifies a progression in fuzzy set structures to effectively address complex scenarios and enhance decision-making processes.

Liu et al. [33] contributed to the field by proposing novel power Muirhead mean AOs tailored for T-SPFSs in their work. Kifayat-Ullah et al. [34] introduced the concept of T-SPF Hamacher AOs with applications in MCDM. Khan et al. [35] extended the domain of T-SPFSs by presenting Schweizer-Sklar power Heronian mean AOs. The consequence of this uniform treatment of MSD, AD, and N-MSD is an undeniably biased final decision. Consequently, there is a recognized necessity for innovative procedures that can appropriately handle MSD, AD, and N-MSD, ensuring a fair and neutral operation of T-SPFN. In our quest for a more robust approach, we introduce two novel procedures designed to handle MSD, AD, and N-MSD impartially. These procedures are grounded in the concept of proportionate distribution constraints for all functions involved in the decision-making process. By adopting these fair procedures, we aim to overcome the biases inherent in existing AOs, providing a more equitable assessment of MSD, AD, and N-MSD.

In their recent works, Riaz et al. [36] contribute significantly to the field of computational intelligence. The study focuses on enhancing green supply chain efficiency by introducing novel linear diophantine fuzzy soft-max AOs, offering a valuable tool for optimizing decisions in environmentally conscious supply chains. Another study [37] addresses the complex issue of MCDM with new similarity measures and TOPSIS method for multi stage decision analysis with cubic intuitionistic fuzzy information. In the realm of multi-criteria decision-making, the authors propose q-rung orthopair fuzzy Aczel–Alsina AOs [38], offering flexibility in handling complex decision scenarios. Additionally, a prior study by Farid and Riaz [39] introduces generalized q-rung orthopair fuzzy Einstein interactive geometric AOs, extending the application of fuzzy logic and providing improved operational laws for handling interactive information in intelligent systems. These contributions collectively advance the theoretical foundations and practical applications of intelligent systems in industrial settings, offering valuable tools for sustainability, modeling, and decision-making. This research addresses crucial applications including sustainability, prequalification assessment, and additive manufacturing, ranging from fuzzy methodologies like Fermatean fuzzy CRITIC-EDAS to conventional CRITIC and EDAS models.

In the recent literature, a notable contribution comes from Jana et al. [40], who proposed a refined interval type-2 fuzzy VIKOR method, offering advancements in decision-making methodologies. Another significant work by Jana et al. [41] delves into the assessment of sustainable strategies for urban parcel delivery, employing a linguistic q-rung orthopair fuzzy Choquet integral approach. Alsattar et al. [42] present an innovative perspective, introducing three-way decision-based conditional probabilities utilizing circular-Pythagorean fuzzy sets. The study focuses on establishing a sustainable smart living framework, incorporating opinion scores and Bayesian rules. Additionally, Jana et al. [43] contribute to the field of multiple attribute group decision-making with their proposed MABAC framework. This logarithmic bipolar fuzzy approach is specifically tailored for supplier selection in complex systems. Overall, these recent studies collectively advance decision-making methodologies and sustainable framework development, showcasing diverse applications in fuzzy systems and intelligent decision support.

Numerous decision-making applications may be found in a variety of sectors, including road segment safety evaluation [44], risk assessment in trade and investment [45], and industrial funds selection [46]. Recent advances in decision-making and computational intelligence have been reported in the literature. Yildirim and Yıldırım [47] presented an innovative way for assessing public happiness with municipal services using the image fuzzy VIKOR method, providing insights for improving local government. Ranjan et al. [48] introduced probabilistic linguistic q-rung orthopair fuzzy Archimedean aggregation operators, which provide enhanced tools for group decision-making in uncertain contexts. Aczel-Alsina aggregation operations based on complicated single-valued neutrosophic information were proposed by Naseem et al. [49], paving the way for dealing with complex decision-making situations. Dastanl [50] assessed the financial performance of energy businesses in the Borsa Istanbul sustainability index using an integrated fuzzy MCDM and trend analysis technique, contributing to the sustainable energy industry. Dinçer et al. [51] developed an innovative fuzzy decision-making model for optimizing renewable energy transition strategies, addressing crucial issues in the shift to sustainable energy sources. Exciting applications linked to efficient risk management in distribution operations [52], and general decision-making [53,54] are covered in the literature. Every contribution gives distinctive insights that help create a thorough understanding of decision support systems across numerous disciplines [58–61]. The MCDM methods used in various fields are shown by Fig. 1. An overview of the many decision-making approaches used in recent literature is provided in this Table 1.

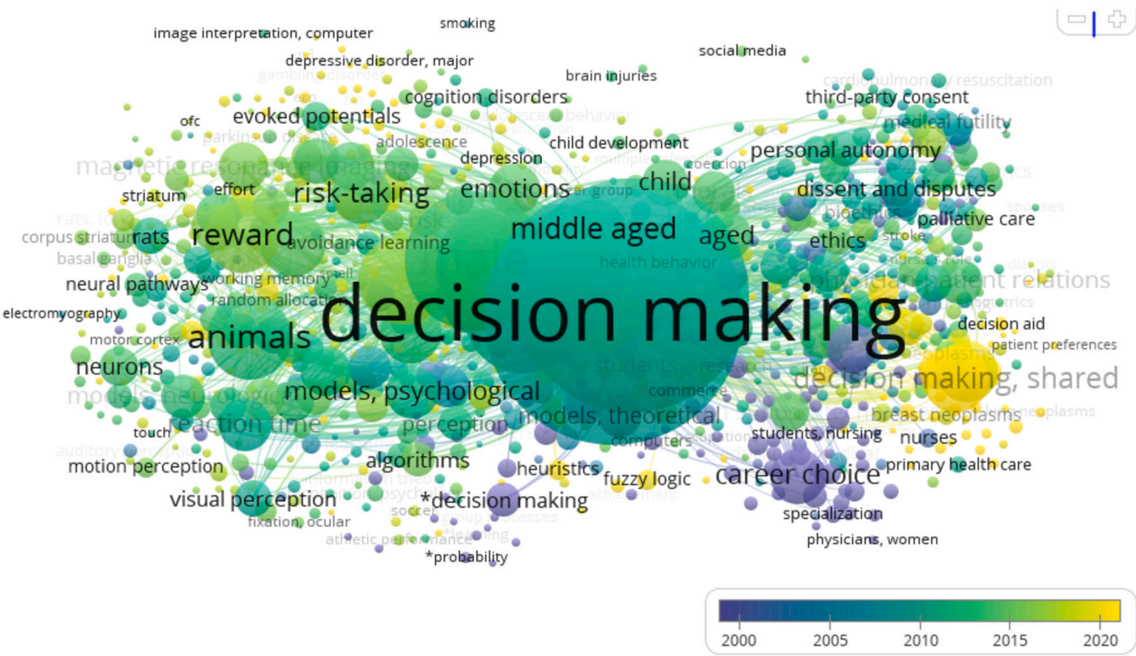

Fig. 1. Working procedure of algorithm.

Table 1
A research overview: techniques and applications.

Author & Year	Technique	Application	Key Findings
Mishra et al. (2022) [55]	Fermatean fuzzy CRITIC-EDAS	Selection of sustainable third-party reverse logistics providers using an improved generalized score function (Journal of Ambient Intelligence and Humanized Computing)	Utilized Fermatean fuzzy CRITIC-EDAS for selecting sustainable reverse logistics providers, enhancing generalized score function.
Naik et al. (2021) [56]	CRITIC and EDAS models	Multi-criteria decision support system for prequalification assessment of construction contractors	Developed a multi-criteria decision support system using CRITIC and EDAS models for prequalifying construction contractors.
Akram et al. (2023) [57]	Linguistic Pythagorean fuzzy CRITIC-EDAS	Multiple-attribute group decision analysis	Proposed a Linguistic Pythagorean fuzzy CRITIC-EDAS method for multiple-attribute group decision analysis.
Menekse et al. (2023) [62]	Pythagorean fuzzy CRITIC EDAS	Additive manufacturing process selection for the automotive industry	Applied Pythagorean fuzzy CRITIC EDAS for additive manufacturing process selection in the automotive industry.
Li et al. (2020) [63]	Interval-valued intuitionistic fuzzy EDAS and CRITIC methods	Evaluating algorithms for the service quality of wireless sensor networks	Evaluated algorithms for wireless sensor network service quality using interval-valued intuitionistic fuzzy EDAS and CRITIC methods.
Öndeş, T., & Özkan, T. (2021) [64]	Integrated CRITIC-EDAS	Financial performance impact of COVID-19 pandemic on the information technology sector	Investigated the financial performance impact of the COVID-19 pandemic on the information technology sector using an integrated CRITIC-EDAS approach.
Sun et al. (2022) [65]	Extended EDAS based on CRITIC method	Multiple attribute decision making in a mixture z-number environment	Proposed an extended EDAS method based on the CRITIC method for multiple attribute decision-making in a mixture z-number environment.
Yalçin, N., & Karakaş, E. (2019) [66]	CRITIC-EDAS	Analysis of corporate sustainability performance	Applied CRITIC-EDAS for the analysis of corporate sustainability performance.

The reviewed literature encompasses a multidimensional exploration of low-carbon scenarios, life-cycle assessments, financing mechanisms, policy effectiveness, and innovation in climate change mitigation. Brutschin et al. [67] contribute a comprehensive feasibility evaluation of low-carbon scenarios, while Hertwich et al. [68] present an integrated life-cycle assessment emphasizing global environmental benefits. Gu et al. [69] investigate the mitigation effects of global low-carbon technology financing and its economic and technological impacts in the context of climate cooperation. Liu et al. [70] focus on the empirical evaluation of a low-carbon city pilot policy in China using a time-varying Difference-in-Differences model, shedding light on the policy's impact on carbon abatement at the city level. Lyu et al. [71] explore the influence of a carbon emission trading system on low-carbon technology innovation, providing insights into the role of market-based mechanisms in driving advancements for carbon reduction. Collectively, these studies contribute to a nuanced understanding of the practicality, environmental implications, financial mechanisms, policy effectiveness, and innovation dynamics associated with low-carbon initiatives.

1.2. Motivation of the manuscript

In recent years, the global energy landscape has witnessed a transformative shift towards sustainability, propelled by advancements in low-carbon technologies and a heightened awareness of environmental issues. This paper is motivated by the recognition of the intricate challenges associated with navigating this transition, specifically in the evaluation of power system reform proposals. As society increasingly prioritizes the need for eco-friendly energy solutions, there arises a critical void in methodologies capable of effectively and precisely assessing reform initiatives within the dynamic context of the power sector. The urgency to bridge this gap is underscored by the realization that without robust evaluation tools tailored to the evolving energy paradigm, the attainment of a more sustainable and environmentally conscious power system remains a formidable task.

1.3. Main contribution

Main contribution of the manuscript is listed as follows.

1. The concept of T-spherical fuzzy sets (T-SFSs) provides a robust optimization approach to deal with uncertainties in the environmental concerns.
2. A wide range of AOs is developed for information analysis and information aggregation.
3. New CRITIC-EDAS framework is proposed which is based on T-spherical fuzzy Dubios-Prade AOs. proposals.
4. A hybrid approach for the power system reforms and advances of low-carbon technology to address environmental concerns as well as transition towards a more sustainable energy infrastructure.
5. Furthermore, the rigorous validation of the proposed methodology through comprehensive analyses, including CRITIC-MAUT, CRITIC-ARAS, CRITIC-EDAS, and CRITIC-MABAC, enhances its practical applicability.

1.4. Structure of the paper

We give a thorough explanation of the underlying ideas necessary to comprehend our topic. In Section 2, we provide a comprehensive illustration of fundamental concepts essential for the understanding of our study. Moving forward, Section 3 is dedicated to the exploration of the Dubios-Prade Operator and its operations, presenting a detailed analysis of its definition, mathematical formulation, and practical applications. In Section 4, our focus shifts to the interactive counterpart, the Dubios-Prade Operator, delving into its extensions and operations within the realm of decision-making processes. Following this, Section 5 introduces an MCDM framework tailored for the recommended Aggregation Operators (AOs), establishing a bridge between theoretical constructs and practical applications. Section 6 takes a practical turn by presenting a numerically detailed test example, providing insights into the real-world implications of our proposed framework. Lastly, Section 7 summarizes the study's significant findings, offering a consolidated overview of key results.

2. Preliminaries

Definition 2.1. [14] Let X be a set. A fuzzy set $\mathcal{F}$ in X is defined as

$$\mathcal{F} = \{(x, \mu(x) : x \in X\}$$

where $\mu(x)$ represent the degree of membership of the element x of X.

Atanasov [15] initiated the idea of IFS as an extension of traditional FSs.

Definition 2.2. [20] A picture fuzzy set A in the universe X is an object in the form of

$$A = \{\langle x, \mu(x), \eta(x), \nu(x) : x \in X\rangle\}$$

where $\mu(x) \in [0,1]$ is called the degree of positive membership (PMD), $\eta(x) \in [0,1]$ is called the degree of neutral membership (NuMD), and $\nu(x) \in [0,1]$ is called the degree of negative membership of each x in A, such that $0 \leq \mu(x) + \eta(x) + \nu(x) \leq 1$ for all $x \in X$.

Definition 2.3. [30–33] A T-SPFS in X is defined in Equation (2.1).

$$\psi = \{\langle \curlyvee, \mu_\psi(\curlyvee), \nu_\psi(\curlyvee), \tau_\psi(\curlyvee) | \curlyvee \in X \rangle\} \tag{2.1}$$

where $\mu_\psi(\curlyvee), \nu_\psi(\curlyvee), \tau_\psi(\curlyvee) \in [0,1]$, such that $0 \le \mu_\psi^t(\curlyvee) + \nu_\psi^t(\curlyvee) + \tau_\psi^t(\curlyvee) \le 1$ for all $\curlyvee \in X$. $\mu_\psi(\curlyvee), \nu_\psi(\curlyvee), \tau_\psi(\curlyvee)$ denote MSD, AD and N-MSD respectively, for some $\curlyvee \in X$.

We denote this pair as $\kappa = (\mu_\kappa, \nu_\kappa, \tau_\kappa)$, throughout this article, and called as T-SPFN with the conditions $\mu_\kappa, \nu_\kappa, \tau_\kappa \in [0,1]$ and $\mu_\kappa^t + \nu_\kappa^t + \tau_\kappa^t \le 1$.

Definition 2.4. [30–33] When implementing T-SPFNs in actual situations, it is crucial to categorize them. For this, "score function" (SF) corresponding to T-SPFN $\kappa = (\mu_\kappa, \nu_\kappa, \tau_\kappa)$ be defined in Equation (2.2).

$$S(\kappa) = \mu_\kappa^t - \tau_\kappa^t \tag{2.2}$$

In many instances, however, the aforesaid function is inadequate for categorizing T-SPFNs under various settings, making it difficult to tell which is better. In Equation (2.3), the accuracy function $\hbar^{\wp}(\kappa)$ is defined as follows

$$\hbar^{\wp}(\kappa) = \mu_\kappa^t + \nu_\kappa^t + \tau_\kappa^t \tag{2.3}$$

We shall provide operational principles for aggregating T-SPFNs.

Definition 2.5. [33] Let $\kappa_1 = \langle \mu_1, \nu_1, \tau_1 \rangle$ and $\kappa_2 = \langle \mu_2, \nu_2, \tau_2 \rangle$ be two T-SPFNs, then

$$\kappa_1 \vee \kappa_2 = \left\langle max\{\mu_1, \mu_2\}, min\{\nu_1, \nu_2\}, min\{\tau_1, \tau_2\} \right\rangle \tag{2.4}$$

$$\kappa_1 \wedge \kappa_2 = \left\langle min\{\mu_1, \mu_2\}, max\{\nu_1, \nu_2\}, max\{\tau_1, \tau_2\} \right\rangle \tag{2.5}$$

Union ($\vee$) and intersection ($\wedge$) are defined in Equation (2.4) and Equation (2.5), respectively.

$$\kappa_1 \oplus \kappa_2 = \left\langle \sqrt[t]{\mu_1^t + \mu_2^t - \mu_1^t \mu_2^t}, \nu_1 \nu_2, \tau_1 \tau_2 \right\rangle \tag{2.6}$$

$$\kappa_1 \otimes \kappa_2 = \left\langle \mu_1 \mu_2, \sqrt[t]{\nu_1^t + \nu_2^t - \nu_1^t \nu_2^t}, \sqrt[t]{\tau_1^t + \tau_2^t - \tau_1^t \tau_2^t} \right\rangle \tag{2.7}$$

Bounded sum ($\oplus$) and bounded product ($\otimes$) are defined in Equation (2.6) and Equation (2.7), respectively.

$$\sigma \kappa_1 = \left\langle \sqrt[t]{1 - (1 - \mu_1^t)^\sigma}, \nu_1^\sigma, \tau_1^\sigma \right\rangle \tag{2.8}$$

$$\kappa_1^\sigma = \left\langle \mu_1^\sigma, \sqrt[t]{1 - (1 - \nu_1^t)^\sigma}, \sqrt[t]{1 - (1 - \tau_1^t)^\sigma} \right\rangle \tag{2.9}$$

Scalar multiplication and power operations are defined in Equation (2.8) and Equation (2.9), respectively.

Definition 2.6. Let $\kappa_1 = \langle \mu_1, \nu_1, \tau_1 \rangle$ and $\kappa_2 = \langle \mu_2, \nu_2, \tau_2 \rangle$ be two T-SPFNs and $\Upsilon, \Upsilon_1, \Upsilon_2 > 0$ be the real numbers, then we have,

1. $\kappa_1 \oplus \kappa_2 = \kappa_2 \oplus \kappa_1$
2. $\kappa_1 \otimes \kappa_2 = \kappa_2 \otimes \kappa_1$
3. $\Upsilon \left(\kappa_1 \oplus \kappa_2\right) = \left(\Upsilon \kappa_1\right) \oplus \left(\Upsilon \kappa_2\right)$
4. $\left(\kappa_1 \otimes \kappa_2\right)^\Upsilon = \kappa_1^\Upsilon \otimes \kappa_2^\Upsilon$
5. $\left(\Upsilon_1 + \Upsilon_2\right) \kappa_1 = \left(\Upsilon_1 \kappa_1\right) \oplus \left(\Upsilon_2 \kappa_2\right)$
6. $\kappa_1^{\Upsilon_1 + \Upsilon_2} = \kappa_1^{\Upsilon_1} \otimes \kappa_2^{\Upsilon_2}$

If $\mu_{\kappa_1} = \nu_{\kappa_1}$ and $\mu_{\kappa_2} = \nu_{\kappa_2}$ then from Definition 2.5 we get, $\mu_{\kappa_1 \oplus \kappa_2} \neq \nu_{\kappa_1 \oplus \kappa_2}, \mu_{\kappa_1 \otimes \kappa_2} \neq \nu_{\kappa_1 \otimes \kappa_2}, \mu_{\Upsilon \kappa_1} \neq \nu_{\Upsilon \kappa_1}, \mu_{\kappa_1^\Upsilon} \neq \nu_{\kappa_1^\Upsilon}$. Thus none of the operations $\kappa_1 \oplus \kappa_2, \kappa_1 \otimes \kappa_2, \Upsilon \kappa_1, \kappa_1^\Upsilon$ found to be neutral or fair indeed. Consequently, our focus must first be on developing fair operations amongst T-SPFNs.

3. Dubios-Prade operator

Definition 3.1. [87] For any two real numbers a, b ∈[0,1], the Dubios-Prade (DP) operator is a t-norm operator, and it is defined as follows:

$$T_{DP}(a,b)=\frac{ab}{max(a,b,p)},\quad (p\in[0,1]) \tag{3.1}$$

its corresponding t-conorm operation is shown as follows:

$$T^*_{DP}(a,b)=1-\frac{(1-a)(1-b)}{max(1-a,1-b,p)},\quad (p\in[0,1]) \tag{3.2}$$

T-norm and T-conorm are shown in Equations (3.1) and Equation (3.2), respectively, where p is a variable parameter. When p changes, the Dubios-Prade operator also changes. When $p=1$, the operator is transformed into the product operator, and when $p=0$ the operator is transformed into the minimum operator.

3.1. DP operations on T-SPFNs

In this section, we construct several basic operations on T-SPFNs and T-SPF Dubios-Prade weighted aggregation (T-SFDPWA) operators. The Dubios-Prade operator plays a pivotal role in MCDM, serving as a valuable tool for combining diverse criteria when evaluating alternative options. In the complex landscape of MCDM, where decision-making involves multiple and often subjective criteria, the Dubios-Prade operator, in conjunction with T-spherical fuzzy sets, adeptly manages the aggregation process by accommodating imprecise or uncertain information. This operator allows decision-makers to take into account essential parameters such as membership degree (MSD), abstinence degree (AD), and non-membership degree (N-MSD), facilitating a more realistic representation of qualitative assessments and expert judgments. Integrating the Dubios-Prade operator into the aggregation phase of MCDM provides the methodology with the flexibility needed to address the inherent uncertainties in decision criteria, contributing to a nuanced and comprehensive evaluation of alternatives based on multiple factors. The use of this approach emphasizes a human-like, natural writing style, with a focus on clarity and authenticity.
Based on the t-norm and t-conorm operations of the DP operators given in Equation (3.1) and Equation (3.2), the T-SFDP operations are defined as follows.

Definition 3.2. Consider $p=\langle\mu_\kappa,\nu_\kappa,\tau_\kappa\rangle$, $\kappa_1=\langle\mu_{\kappa_1},\nu_{\kappa_1},\tau_{\kappa_1}\rangle$ and $\kappa_2=\langle\mu_{\kappa_2},\nu_{\kappa_2},\tau_{\kappa_2}\rangle$ be the three T-SPFNs and $\gamma>0$.

$$\kappa_1\tilde{\oplus}_{DP}\kappa_2=\left(\begin{array}{l}\sqrt[t]{\left(1-\frac{(1-\mu^t{}_{\kappa_1})(1-\mu^t{}_{\kappa_2})}{max\{1-\mu^t{}_{\kappa_1},1-\mu^t{}_{\kappa_2},p\}}\right)},\\ \sqrt[t]{\left(\frac{\nu^t{}_{\kappa_1}\nu^t{}_{\kappa_2}}{max\{\nu^t{}_{\kappa_1},\nu^t{}_{\kappa_2},p\}}\right)},\\ \sqrt[t]{\left(\frac{\tau^t{}_{\kappa_1}\tau^t{}_{\kappa_2}}{max\{\tau^t{}_{\kappa_1},\tau^t{}_{\kappa_2},p\}}\right)}\end{array}\right) \tag{3.3}$$

$$\kappa_1\tilde{\otimes}_{DP}\kappa_2=\left(\begin{array}{l}\sqrt[t]{\left(\frac{\mu^t{}_{\kappa_1}\mu^t{}_{\kappa_2}}{max\{\mu^t{}_{\kappa_1},\mu^t{}_{\kappa_2},p\}}\right)},\\ \sqrt[t]{\left(1-\frac{(1-\nu^t{}_{\kappa_1})(1-\nu^t{}_{\kappa_2})}{max\{1-\nu^t{}_{\kappa_1},1-\nu^t{}_{\kappa_2},p\}}\right)},\\ \sqrt[t]{\left(\frac{\tau^t{}_{\kappa_1}\tau^t{}_{\kappa_2}}{max\{\tau^t{}_{\kappa_1},\tau^t{}_{\kappa_2},p\}}\right)}\end{array}\right) \tag{3.4}$$

Bounded sum ($\tilde{\oplus}_{DP}$) and bounded product ($\tilde{\otimes}_{DP}$) using t-conorm and t-norm are shown in Equation (3.3) and Equation (3.4), respectively.

$$\gamma*\kappa=\left(\begin{array}{l}\sqrt[t]{\left(1-\frac{(1-\mu^t{}_{\kappa})^\gamma}{(max\{1-\mu^t{}_{\kappa},p\})^{\gamma-1}}\right)},\\ \sqrt[t]{\left(\frac{\nu^{t\gamma}{}_{\kappa}}{max(\{\nu^t{}_{\kappa},p\})^{\gamma-1}}\right)},\\ \sqrt[t]{\left(\frac{\tau^{t\gamma}{}_{\kappa}}{(max\{\tau^t{}_{\kappa},p\})^{\gamma-1}}\right)}\end{array}\right) \tag{3.5}$$

$$\kappa^{\gamma}=\left(\begin{array}{c}\sqrt[t]{\left(\frac{{\mu^{t}}_{\kappa}^{\gamma}}{max(\{\mu^{t}{}_{\kappa},p\})^{\gamma}-1}\right)},\\ \sqrt[t]{\left(1-\frac{(1-\nu^{t}{}_{\kappa})^{\gamma}}{(max\{1-\nu^{t}{}_{\kappa},p\})^{\gamma}-1}\right)},\\ \sqrt[t]{\left(\frac{{\tau^{t}}_{\kappa}^{\gamma}}{(max\{\tau^{t}{}_{\kappa},p\})^{\gamma}-1}\right)}\end{array}\right) \tag{3.6}$$

Scalar multiplication and power operations defined using t-conorm and t-norm are shown in Equation (3.5) and Equation (3.6), respectively. It can be verified that the T-SFDP addition and product operations defined in this section satisfy the rules of t-conorms and t-norms. Additionally, the multiplication and power operations satisfy the rules of t-conorms and t-norms.

3.2. T-SFDPWA operators

Definition 3.3. Let $\kappa_i=\langle\mu_{\alpha_{(i)}},\nu_{\alpha_{(i)}},\tau_{\alpha_{(i)}}\rangle$ be the collection of T-SPFNs. The T-SFDPWA: $R^n\rightarrow R$ be the mapping shown in Equation (3.7).

$$\text{T-SFDPWA}(\kappa_1,\kappa_2,\dots\kappa_e)=\left(\vartheta_1*\kappa_1\oplus\tilde{_{IDP}}\vartheta_2*\kappa_2\oplus\tilde{_{IDP}}\dots,\oplus\tilde{_{IDP}}\vartheta_e*\kappa_e\right) \tag{3.7}$$

then the mapping T-SFDPWA is called “T-spherical fuzzy Dubios-Prade weighted averaging (T-SFDPWA) operator”, here $w=(\vartheta_1,...,\vartheta_e)$ is the weight vector (WV) of $\kappa_{(i)}$ with $\vartheta_i>0$ and $\sum_{i=1}^{e}\vartheta_i=1$.

We may also investigate T-SFDPWA using proposed operational rules, as demonstrated in the next theorem.

Theorem 3.4. *Let $\kappa_i=\langle\mu_{\alpha_i},\nu_{\alpha_i},\tau_{\alpha_i}\rangle$ be the collection of T-SPFNs. The T-SFDPWA can is defined in Equation (3.8).*

$$\text{T-SFDPWA}(\kappa_1,\kappa_2,\dots,\kappa_e)=\left(\begin{array}{c}\sqrt[t]{1-\frac{\Pi_{i=1}^{n}\frac{(1-\mu_{\alpha_i}{}^{t})^{\vartheta_i}}{(max\{1-\mu_{\alpha_i}{}^{t},p\})^{\vartheta_i-1}}}{\Pi_{i=1}^{n-1}max\{1-\mu_{\alpha_i}{}^{t},p\}}},\\ \sqrt[t]{\frac{\Pi_{i=1}^{n}\frac{(\nu_{\alpha_i}{}^{t})^{\vartheta_i}}{(max\{\nu_{\alpha_i}{}^{t},p\})^{\vartheta_i-1}}}{\Pi_{i=1}^{n-1}max\{1-\nu_{\alpha_i}{}^{t},p\}}},\\ \sqrt[t]{\frac{\Pi_{i=1}^{n}\frac{(\tau_{\alpha_i}{}^{t})^{\vartheta_i}}{(max\{\tau_{\alpha_i}{}^{t},p\})^{\vartheta_i-1}}}{\Pi_{i=1}^{n-1}max\{1-\tau_{\alpha_i}{}^{t},p\}}}\end{array}\right) \tag{3.8}$$

where ϑ_i is the WV of $\kappa_{(i)}$ with $\vartheta_i>0$ and $\sum_{i=1}^{e}\vartheta_i=1$.

Moreover, in Equation (4.12), if there is a T-SPFN with a N-MSD value of zero, the resulting N-MSD from the T-SFDPWA operator will consistently remain zero, regardless of any variations in the other T-SPFNs or the weight vector. To better understand this issue, refer to Example 3.5 for a visual demonstration. Upon further analysis, it has come to our attention that the outcomes of the T-SFDP operations and the T-SFDPWA operator's aggregations may not meet our expectations, particularly when dealing with extreme data values such as 0s in the T-SPFNs. This lack of satisfaction primarily stems from the fact that the relationship between MSDs and N-MSDs is not adequately portrayed. When examining Equations (3.3) - (3.6), it becomes evident that the MSD and N-MSD act independently during the T-SFDP procedures, implying that alterations in one do not affect the other.

Example 3.5. Suppose that $a_1=\langle 0.72,0,0.24\rangle$, $a_2=\langle 0.43,0.32,0.42\rangle$ and $a_3=\langle 0.57,0.43,0.34\rangle$ are three T-SPFNs, and the weight vector is $w=\langle 0.43,0,0.32.25\rangle$. Using the T-SFDPWA operator with $t=3$ and $p=3$, the aggregation result of $T-SFDPWA(a_1,a_2,a_3)=\langle 0.606,0,0.42.31316\rangle$.

4. Interactive Dubios-Prade operator

To focus on the problem of T-SFDP in this section and study the implementation of T-SPFIDP operations as well as the utilization of the T-SFIDPWA operator. Additionally, a group decision-making approach that relies on the T-SFIDPWA operator is illustrated.

Definition 4.1. Consider $p=\langle\mu_\kappa,\nu_\kappa,\tau_\kappa\rangle$, $\kappa_1=\left\langle\mu_{\kappa_1},\nu_{\kappa_1},\tau_{\kappa_1}\right\rangle$ and $\kappa_2=\left\langle\mu_{\kappa_2},\nu_{\kappa_2},\tau_{\kappa_2}\right\rangle$ be the three T-SPFNs and $\gamma>0$. Then T-SPFIDP operations are defined.

$$\kappa_1 \tilde{\oplus}_{IDP} \kappa_2 = \left(\begin{array}{l} \sqrt[t]{\left(1 - \frac{(1-\mu^t{}_{\kappa_1})(1-\mu^t{}_{\kappa_2})}{max\{1-\mu^t{}_{\kappa_1}, 1-\mu^t{}_{\kappa_2}, p\}}\right)}, \\ \sqrt[t]{\left(\frac{(1-\mu^t{}_{\kappa_1})(1-\mu^t{}_{\kappa_2})-(1-\mu^t{}_{\kappa_1}-\nu^t{}_{\kappa_1})-(1-\mu^t{}_{\kappa_2}-\nu^t{}_{\kappa_2})}{max\{1-\mu^t{}_{\kappa_1}, 1-\mu^t{}_{\kappa_2}, p\}}\right)}, \\ \sqrt[t]{\left(\frac{(1-\mu^t{}_{\kappa_1})(1-\mu^t{}_{\kappa_2})-(1-\mu^t{}_{\kappa_1}-\tau^t{}_{\kappa_1})-(1-\mu^t{}_{\kappa_2}-\tau^t{}_{\kappa_2})}{max\{1-\mu^t{}_{\kappa_1}, 1-\mu^t{}_{\kappa_2}, p\}}\right)} \end{array} \right) \tag{4.1}$$

$$\kappa_1 \tilde{\otimes}_{IDP} \kappa_2 = \left(\begin{array}{l} \sqrt[t]{\left(\frac{(1-\nu^t{}_{\kappa_1})(1-\nu^t{}_{\kappa_2})-(1-\nu^t{}_{\kappa_2}-\mu^t{}_{\kappa_1})-(1-\nu^t{}_{\kappa_2}-\mu^t{}_{\kappa_2})}{max\{1-\nu^t{}_{\kappa_1}, 1-\nu^t{}_{\kappa_2}, p\}}\right)}, \\ \sqrt[t]{\left(1 - \frac{(1-\nu^t{}_{\kappa_1})(1-\nu^t{}_{\kappa_2})}{max\{1-\nu^t{}_{\kappa_1}, 1-\nu^t{}_{\kappa_2}, p\}}\right)}, \\ \sqrt[t]{\left(\frac{(1-\nu^t{}_{\kappa_1})(1-\nu^t{}_{\kappa_2})-(1-\nu^t{}_{\kappa_2}-\tau^t{}_{\kappa_1})-(1-\nu^t{}_{\kappa_2}-\tau^t{}_{\kappa_2})}{max\{1-\nu^t{}_{\kappa_1}, 1-\nu^t{}_{\kappa_2}, p\}}\right)} \end{array} \right) \tag{4.2}$$

Bounded sum and bounded product operations for the T-SFIDPWA operator defined using t-conorm and t-norm are shown in Equation (4.1) and Equation (4.2), respectively.

$$\gamma * \kappa = \left(\begin{array}{l} \sqrt[t]{\left(1 - \frac{(1-\mu^t{}_{\kappa})^{\gamma}}{(max\{1-\mu^t{}_{\kappa}, p\})^{\gamma}-1}\right)}, \\ \sqrt[t]{\left(\frac{(1-\mu^t{}_{\kappa})^{\gamma}-(1-\mu^t{}_{\kappa}-\nu^t{}_{\kappa})}{(max\{1-\mu^t{}_{\kappa}, p\})^{\gamma}-1}\right)}, \\ \sqrt[t]{\left(\frac{(1-\mu^t{}_{\kappa})^{\gamma}-(1-\mu^t{}_{\kappa}-\tau^t{}_{\kappa})}{(max\{1-\mu^t{}_{\kappa}, p\})^{\gamma}-1}\right)} \end{array} \right) \tag{4.3}$$

$$\kappa^{\gamma} = \left(\begin{array}{l} \sqrt[t]{\left(\frac{(1-\nu^t{}_{\kappa})^{\gamma}-(1-\nu^t{}_{\kappa}-\mu^t{}_{\kappa})}{(max\{1-\nu^t{}_{\kappa}, p\})^{\gamma}-1}\right)}, \\ \sqrt[t]{\left(1 - \frac{(1-\nu^t{}_{\kappa})^{\gamma}}{(max\{1-\nu^t{}_{\kappa}, p\})^{\gamma}-1}\right)}, \\ \sqrt[t]{\left(\frac{(1-\nu^t{}_{\kappa})^{\gamma}-(1-\nu^t{}_{\kappa}-\tau^t{}_{\kappa})}{(max\{1-\nu^t{}_{\kappa}, p\})^{\gamma}-1}\right)} \end{array} \right) \tag{4.4}$$

Scalar multiplication and power operations for the T-SFIDPWA operator defined using t-conorm and t-norm are shown in Equation (4.3) and Equation (4.4), respectively. It can be verified that the results of the T-SPFIDP operations are still T-SPFNs.

Theorem 4.2. *Consider* $p = \langle \mu_\kappa, \nu_\kappa, \tau_\kappa \rangle$, $\kappa_1 = \left\langle \mu_{\kappa_1}, \nu_{\kappa_1}, \tau_{\kappa_1} \right\rangle$ *and* $\kappa_2 = \left\langle \mu_{\kappa_2}, \nu_{\kappa_2}, \tau_{\kappa_2} \right\rangle$ *be the three T-SPFNs,* $t > 2$ *and* γ*,* γ_1*,* $\gamma_2 > 0$*. Then T-SPFIDP operations satisfy the following six properties.*

Commutative law of addition:

$$\kappa_1 \oplus_{IDP} \kappa_2 = \kappa_2 \oplus_{IDP} \kappa_1 \tag{4.5}$$

Commutative law of multiplication:

$$\kappa_1 \otimes_{IDP} \kappa_2 = \kappa_2 \otimes_{IDP} \kappa_1 \tag{4.6}$$

The commutative law of addition and the commutative law of multiplication is shown in Equation (4.5) and Equation (4.6).
Distributive law of multiplication:

$$\gamma(\kappa_1 \oplus_{IDP} \kappa_2) = (\gamma\kappa_2) \oplus_{IDP} (\gamma\kappa_1) \tag{4.7}$$

Distribution law of power:

$$(\kappa_1 \otimes_{IDP} \kappa_2)^{\gamma} = (\kappa_2)^{\gamma} \otimes_{IDP} (\kappa_1)^{\gamma} \tag{4.8}$$

The distributive law of multiplication and the distribution law of power is shown in Equation (4.7) and Equation (4.8).
Associative law of multiplication:

$$(\gamma_1\kappa)\oplus_{IDP}(\gamma_2\kappa)=(\gamma_1+\gamma_2)\kappa \tag{4.9}$$

Associative law of power:

$$(\kappa_1^{\gamma})\otimes_{IDP}(\kappa_2^{\gamma})=\kappa^{(\gamma_1+\gamma_2)} \tag{4.10}$$

The associative law of multiplication and the associative law of power is shown in Equation (4.9) and Equation (4.10). All theorems can be proven using the T-SPFIDP operations. This paper exclusively provides the proof for Equation (4.7).

Proof. From the Equation (4.1) and Equation (4.3), we have that

$$(\gamma\kappa_1)\oplus_{IDP}(\gamma\kappa_2)=\begin{pmatrix}\sqrt[t]{\left(1-\frac{(1-\mu^t{}_{\kappa_1})^{\gamma}}{(max\{1-\mu^t{}_{\kappa_1},p\})^{\gamma}-1}\right)},\\ \sqrt[t]{\left(\frac{(1-\mu^t{}_{\kappa_1})^{\gamma}-(1-\mu^t{}_{\kappa_1}-v^t{}_{\kappa_1})}{(max\{1-\mu^t{}_{\kappa_1},p\})^{\gamma}-1}\right)},\\ \sqrt[t]{\left(\frac{(1-\mu^t{}_{\kappa_1})^{\gamma}-(1-\mu^t{}_{\kappa_1}-\tau^t{}_{\kappa_1})}{(max\{1-\mu^t{}_{\kappa_1},p\})^{\gamma}-1}\right)}\end{pmatrix}\oplus\begin{pmatrix}\sqrt[t]{\left(1-\frac{(1-\mu^t{}_{\kappa_2})^{\gamma}}{(max\{1-\mu^t{}_{\kappa_2},p\})^{\gamma}-1}\right)},\\ \sqrt[t]{\left(\frac{(1-\mu^t{}_{\kappa_2})^{\gamma}-(1-\mu^t{}_{\kappa_2}-v^t{}_{\kappa_2})}{(max\{1-\mu^t{}_{\kappa_2},p\})^{\gamma}-1}\right)},\\ \sqrt[t]{\left(\frac{(1-\mu^t{}_{\kappa_2})^{\gamma}-(1-\mu^t{}_{\kappa_2}-\tau^t{}_{\kappa_2})}{(max\{1-\mu^t{}_{\kappa_2},p\})^{\gamma}-1}\right)}\end{pmatrix}$$

$$=\begin{pmatrix}\sqrt[t]{\left(1-\frac{\left(\frac{(1-\mu^t{}_{\kappa_1})^{\gamma}}{(max\{1-\mu^t{}_{\kappa_1},p\})^{\gamma}-1}\right)\left(\frac{(1-\mu^t{}_{\kappa_2})^{\gamma}}{(max\{1-\mu^t{}_{\kappa_2},p\})^{\gamma}-1}\right)}{max\left\{\left(\frac{(1-\mu^t{}_{\kappa_1})^{\gamma}}{(max\{1-\mu^t{}_{\kappa_1},p\})^{\gamma}-1}\right)\left(\frac{(1-\mu^t{}_{\kappa_2})^{\gamma}}{(max\{1-\mu^t{}_{\kappa_2},p\})^{\gamma}-1}\right),p\right\}}\right)},\\ \sqrt[t]{\left(\frac{\left(\frac{(1-\mu^t{}_{\kappa_1})^{\gamma}}{(max\{1-\mu^t{}_{\kappa_1},p\})^{\gamma}-1}\right)\left(\frac{(1-\mu^t{}_{\kappa_2})^{\gamma}}{(max\{1-\mu^t{}_{\kappa_2},p\})^{\gamma}-1}\right)-\left(\frac{(1-\mu^t{}_{\kappa_1}-v_{\kappa_1})^{\gamma}}{(max\{1-\mu^t{}_{\kappa_1},p\})^{\gamma}-1}\right)\left(\frac{(1-\mu^t{}_{\kappa_2}-v_{\kappa_2})^{\gamma}}{(max\{1-\mu^t{}_{\kappa_2},p\})^{\gamma}-1}\right)}{max\left\{\left(\frac{(1-\mu^t{}_{\kappa_1})^{\gamma}}{(max\{1-\mu^t{}_{\kappa_1},p\})^{\gamma}-1}\right)\left(\frac{(1-\mu^t{}_{\kappa_2})^{\gamma}}{(max\{1-\mu^t{}_{\kappa_2},p\})^{\gamma}-1}\right),p\right\}}\right)},\\ \sqrt[t]{\left(\frac{\left(\frac{(1-\mu^t{}_{\kappa_1})^{\gamma}}{(max\{1-\mu^t{}_{\kappa_1},p\})^{\gamma}-1}\right)\left(\frac{(1-\mu^t{}_{\kappa_2})^{\gamma}}{(max\{1-\mu^t{}_{\kappa_2},p\})^{\gamma}-1}\right)-\left(\frac{(1-\mu^t{}_{\kappa_1}-\tau_{\kappa_1})^{\gamma}}{(max\{1-\mu^t{}_{\kappa_1},p\})^{\gamma}-1}\right)\left(\frac{(1-\mu^t{}_{\kappa_2}-\tau_{\kappa_2})^{\gamma}}{(max\{1-\mu^t{}_{\kappa_2},p\})^{\gamma}-1}\right)}{max\left\{\left(\frac{(1-\mu^t{}_{\kappa_1})^{\gamma}}{(max\{1-\mu^t{}_{\kappa_1},p\})^{\gamma}-1}\right)\left(\frac{(1-\mu^t{}_{\kappa_2})^{\gamma}}{(max\{1-\mu^t{}_{\kappa_2},p\})^{\gamma}-1}\right),p\right\}}\right)}\end{pmatrix}$$

$$=\gamma\begin{pmatrix}\sqrt[t]{\left(1-\frac{(1-\mu^t{}_{\kappa_1})(1-\mu^t{}_{\kappa_2})}{max\{1-\mu^t{}_{\kappa_1},1-\mu^t{}_{\kappa_2},p\}}\right)},\\ \sqrt[t]{\left(\frac{(1-\mu^t{}_{\kappa_1})(1-\mu^t{}_{\kappa_2})-(1-\mu^t{}_{\kappa_1}-v^t{}_{\kappa_1})-(1-\mu^t{}_{\kappa_2}-v^t{}_{\kappa_2})}{max\{1-\mu^t{}_{\kappa_1},1-\mu^t{}_{\kappa_2},p\}}\right)},\\ \sqrt[t]{\left(\frac{(1-\mu^t{}_{\kappa_1})(1-\mu^t{}_{\kappa_2})-(1-\mu^t{}_{\kappa_1}-\tau^t{}_{\kappa_1})-(1-\mu^t{}_{\kappa_2}-\tau^t{}_{\kappa_2})}{max\{1-\mu^t{}_{\kappa_1},1-\mu^t{}_{\kappa_2},p\}}\right)})\end{pmatrix}$$

$$=\gamma\left(\kappa_1\tilde{\oplus}_{IDP}\kappa_2\right)\quad\square$$

4.1. T-SFIDPWA operators

Definition 4.3. Let $\kappa_i=\langle\mu_{\alpha_{(i)}},v_{\alpha_{(i)}},\tau_{\alpha_{(i)}}\rangle$ be the collection of T-SPFNs. Then T-SFIDPWA: $R^n\to R$, be the mapping shown in Equation (4.11).

$$\text{T-SFIDPWA}(\kappa_1,\kappa_2,\ldots\kappa_e)=\left(\vartheta_1*\kappa_1\tilde{\oplus}_{IDP}\vartheta_2*\kappa_2\tilde{\oplus}_{IDP}\ldots,\tilde{\oplus}_{IDP}\vartheta_e*\kappa_e\right) \tag{4.11}$$

then the mapping T-SFIDPWA is called “T-spherical fuzzy interactive Dubois–Prade weighted averaging (T-SFIDPWA) operator”, here ϑ_i is the weight vector (WV) of $\kappa_{(i)}$ with $\vartheta_i>0$ and $\sum_{i=1}^{e}\vartheta_i=1$.

We may also investigate T-SFIDPWA using proposed operational rules, as demonstrated in the theorem.

Theorem 4.4. *Let $\kappa_i = \langle \mu_{\alpha_i}, \nu_{\alpha_i}, \tau_{\alpha_i} \rangle$ be the collection of T-SPFNs, then T-SFIDPWA shows in Equation (4.12).*

$$\text{T-SFIDPWA}(\kappa_1, \kappa_2, \ldots, \kappa_e) = \left(\begin{array}{c} \sqrt[t]{1 - \dfrac{\prod_{i=1}^{n} \frac{(1-\mu_{\alpha_i}{}^t)^{\vartheta_i}}{(max\{1-\mu_{\alpha_i}{}^t, p\})^{\vartheta_i - 1}}}{\prod_{i=1}^{n-1}(max\{1-\mu_{\alpha_i}{}^t, p\})}}, \\ \sqrt[t]{\dfrac{\frac{\prod_{i=1}^{n}(1-\mu^t{}_{\alpha_i})^{\vartheta_i} - \prod_{i=1}^{n}(1-\mu^t{}_{\alpha_i} - v^t{}_{\alpha_i})^{\vartheta_i}}{\prod_{i=1}^{n}(max\{1-\mu_{\alpha_i}{}^t, p\})^{\vartheta_i - 1}}}{\prod_{i=1}^{n-1}(max\{1-\mu_{\alpha_i}{}^t, p\})}}, \\ \sqrt[t]{\dfrac{\frac{\prod_{i=1}^{n}(1-\mu^t{}_{\alpha_i})^{\vartheta_i} - \prod_{i=1}^{n}(1-\mu^t{}_{\alpha_i} - \tau^t{}_{\alpha_i})^{\vartheta_i}}{\prod_{i=1}^{n}(max\{1-\mu_{\alpha_i}{}^t, p\})^{\vartheta_i - 1}}}{\prod_{i=1}^{n-1}(max\{1-\mu_{\alpha_i}{}^t, p\})}} \end{array} \right) \tag{4.12}$$

where ϑ_i is the WV of $\kappa_{(i)}$ with $\vartheta_i > 0$ and $\sum_{i=1}^{e} \vartheta_i = 1$.

Proof. Theorem 4.4 can be proven by mathematical induction.
for $n = 2$ we have

$$\vartheta_1^{\gamma} * \kappa_2 = \left(\begin{array}{c} \sqrt[t]{\left(1 - \dfrac{(1-\mu^t{}_{\alpha_1})^{\vartheta_1}}{(max\{1-\mu^t{}_{\alpha_1}, p\})^{\vartheta_1 - 1}}\right)}, \\ \sqrt[t]{\left(\dfrac{(1-\mu^t{}_{\alpha_1})^{\vartheta_1} - (1-\mu^t{}_{\alpha_1} - v^t{}_{\alpha_1})}{(max\{1-\mu^t{}_{\alpha_1}, p\})^{\vartheta_1 - 1}}\right)}, \\ \sqrt[t]{\left(\dfrac{(1-\mu^t{}_{\alpha_1})^{\vartheta_1} - (1-\mu^t{}_{\alpha_1} - \tau^t{}_{\alpha_1})}{(max\{1-\mu^t{}_{\alpha_1}, p\})^{\vartheta_i - 1}}\right)} \end{array} \right)$$

$$\vartheta_2^{\gamma} * \kappa_2 = \left(\begin{array}{c} \sqrt[t]{\left(1 - \dfrac{(1-\mu^t{}_{\alpha_2})^{\vartheta_2}}{(max\{1-\mu^t{}_{\alpha_2}, p\})^{\vartheta_2 - 1}}\right)}, \\ \sqrt[t]{\left(\dfrac{(1-\mu^t{}_{\alpha_2})^{\vartheta_2} - (1-\mu^t{}_{\alpha_2} - v^t{}_{\alpha_2})}{(max\{1-\mu^t{}_{\alpha_2}, p\})^{\vartheta_2 - 1}}\right)}, \\ \sqrt[t]{\left(\dfrac{(1-\mu^t{}_{\alpha_2})^{\vartheta_2} - (1-\mu^t{}_{\alpha_2} - \tau^t{}_{\alpha_2})}{(max\{1-\mu^t{}_{\alpha_2}, p\})^{\vartheta_2 - 1}}\right)} \end{array} \right)$$

$$\text{T-SFIDPWA}(\kappa_1, \kappa_2) = \left(\begin{array}{c} \sqrt[t]{\left(1 - \dfrac{\left(\frac{(1-\mu^t{}_{\alpha_1})^{\vartheta_1}}{(max\{1-\mu^t{}_{\alpha_1}, p\})^{\vartheta_1 - 1}}\right)\left(\frac{(1-\mu^t{}_{\alpha_2})^{\vartheta_2}}{(max\{1-\mu^t{}_{\alpha_2}, p\})^{\vartheta_2 - 1}}\right)}{max\left\{\left(\frac{(1-\mu^t{}_{\alpha_1})^{\vartheta_1}}{(max\{1-\mu^t{}_{\alpha_1}, p\})^{\vartheta_1 - 1}}\right)\left(\frac{(1-\mu^t{}_{\alpha_2})^{\vartheta_2}}{(max\{1-\mu^t{}_{\alpha_2}, p\})^{\vartheta_2 - 1}}\right), p\right\}}\right)}, \\ \sqrt[t]{\left(\dfrac{\left(\frac{(1-\mu^t{}_{\alpha_1})^{\vartheta_1}}{(max\{1-\mu^t{}_{\alpha_1}, p\})^{\vartheta_1 - 1}}\right)\left(\frac{(1-\mu^t{}_{\alpha_2})^{\vartheta_2}}{(max\{1-\mu^t{}_{\alpha_2}, p\})^{\vartheta_2 - 1}}\right) - \left(\frac{(1-\mu^t{}_{\alpha_1} - v_{\alpha_1})^{\vartheta_2}}{(max\{1-\mu^t{}_{\alpha_1}, p\})^{\vartheta_1 - 1}}\right)\left(\frac{(1-\mu^t{}_{\alpha_2} - v_{\alpha_2})^{\vartheta_2}}{(max\{1-\mu^t{}_{\alpha_2}, p\})^{\vartheta_2 - 1}}\right)}{max\left\{\left(\frac{(1-\mu^t{}_{\alpha_1})^{\vartheta_1}}{(max\{1-\mu^t{}_{\alpha_1}, p\})^{\vartheta_1 - 1}}\right)\left(\frac{(1-\mu^t{}_{\alpha_2})^{\vartheta_1}}{(max\{1-\mu^t{}_{\alpha_2}, p\})^{\vartheta_2 - 1}}\right), p\right\}}\right)}, \\ \sqrt[t]{\left(\dfrac{\left(\frac{(1-\mu^t{}_{\alpha_1})^{\vartheta_1}}{(max\{1-\mu^t{}_{\alpha_1}, p\})^{\vartheta_1 - 1}}\right)\left(\frac{(1-\mu^t{}_{\alpha_2})^{\vartheta_2}}{(max\{1-\mu^t{}_{\alpha_2}, p\})^{\vartheta_2 - 1}}\right) - \left(\frac{(1-\mu^t{}_{\alpha_1} - \tau_{\alpha_1})^{\vartheta_1}}{(max\{1-\mu^t{}_{\alpha_1}, p\})^{\vartheta_1 - 1}}\right)\left(\frac{(1-\mu^t{}_{\alpha_2} - \tau_{\alpha_2})^{\vartheta_2}}{(max\{1-\mu^t{}_{\alpha_2}, p\})^{\vartheta_2 - 1}}\right)}{max\left\{\left(\frac{(1-\mu^t{}_{\alpha_1})^{\vartheta_1}}{(max\{1-\mu^t{}_{\alpha_1}, p\})^{\vartheta_1 - 1}}\right)\left(\frac{(1-\mu^t{}_{\alpha_2})^{\vartheta_2}}{(max\{1-\mu^t{}_{\alpha_2}, p\})^{\vartheta_2 - 1}}\right), p\right\}}\right)} \end{array} \right)$$

$$= \left(\begin{array}{c} \sqrt[t]{1 - \dfrac{\prod_{i=1}^{2} \frac{(1-\mu_{\alpha_i}{}^t)^{\vartheta_i}}{(max\{1-\mu_{\alpha_i}{}^t, p\})^{\vartheta_i - 1}}}{\prod_{i=1}^{2-1}(max\{1-\mu_{\alpha_i}{}^t, p\})}}, \\ \sqrt[t]{\dfrac{\frac{\prod_{i=1}^{2}(1-\mu^t{}_{\alpha_i})^{\vartheta_i} - \prod_{i=1}^{2}(1-\mu^t{}_{\alpha_i} - v^t{}_{\alpha_i})^{\vartheta_i}}{\prod_{i=1}^{2}(max\{1-\mu_{\alpha_i}{}^t, p\})^{\vartheta_i - 1}}}{(max\{1-\mu_{\alpha_i}{}^t, p\})}}, \\ \sqrt[t]{\dfrac{\frac{\prod_{i=1}^{2}(1-\mu^t{}_{\alpha_i})^{\vartheta_i} - \prod_{i=1}^{2}(1-\mu^t{}_{\alpha_i} - \tau^t{}_{\alpha_i})^{\vartheta_i}}{\prod_{i=1}^{2}(max\{1-\mu_{\alpha_i}{}^t, p\})^{\vartheta_i - 1}}}{(max\{1-\mu_{\alpha_i}{}^t, p\})}} \end{array} \right)$$

This shows that Equation 4.4 hold for $n=2$ and assuming that Equation 4.4 hold for $n=k$, then we have

$$\text{T-SFIDPWA}(\kappa_1,\kappa_2,\dots,\kappa_k)=\left(\begin{array}{c}\sqrt[t]{1-\dfrac{\Pi_{i=1}^{k}\frac{(1-\mu_{\alpha_i}{}^{t})^{\vartheta_i}}{(max\{1-\mu_{\alpha_i}{}^{t},p\})^{\vartheta_i-1}}}{\Pi_{i=1}^{k-1}(max\{1-\mu_{\alpha_i}{}^{t},p\})}},\\ \sqrt[t]{\dfrac{\frac{\Pi_{i=1}^{k}(1-\mu^{t}_{\alpha_i})^{\vartheta_i}-\Pi_{i=1}^{k}(1-\mu^{t}{}_{\alpha_i}-\nu^{t}{}_{\alpha_i})^{\vartheta_i}}{\Pi_{i=1}^{k}(max\{1-\mu_{\alpha_i}{}^{t},p\})^{\vartheta_i-1}}}{\Pi_{i=1}^{k-1}(max\{1-\mu_{\alpha_i}{}^{t},p\})}},\\ \sqrt[t]{\dfrac{\frac{\Pi_{i=1}^{k}(1-\mu^{t}_{\alpha_i})^{\vartheta_i}-\Pi_{i=1}^{k}(1-\mu^{t}{}_{\alpha_i}-\tau^{t}{}_{\alpha_i})^{\vartheta_i}}{\Pi_{i=1}^{k}(max\{1-\mu_{\alpha_i}{}^{t},p\})^{\vartheta_i-1}}}{\Pi_{i=1}^{k-1}(max\{1-\mu_{\alpha_i}{}^{t},p\})}}\end{array}\right)$$

When $n=k+1$, we have

$$\begin{aligned}&\text{T-SFIDPWA}(\kappa_1,\kappa_2,\dots,\kappa_k,\kappa_{k+1})\\ &=\left(\begin{array}{c}\sqrt[t]{1-\dfrac{\Pi_{i=1}^{k}\frac{(1-\mu_{\alpha_i}{}^{t})^{\vartheta_i}}{(max\{1-\mu_{\alpha_i}{}^{t},p\})^{\vartheta_i-1}}}{\Pi_{i=1}^{k-1}(max\{1-\mu_{\alpha_i}{}^{t},p\})}},\\ \sqrt[t]{\dfrac{\frac{\Pi_{i=1}^{k}(1-\mu^{t}_{\alpha_i})^{\vartheta_i}-\Pi_{i=1}^{k}(1-\mu^{t}{}_{\alpha_i}-\nu^{t}{}_{\alpha_i})^{\vartheta_i}}{\Pi_{i=1}^{k}(max\{1-\mu_{\alpha_i}{}^{t},p\})^{\vartheta_i-1}}}{\Pi_{i=1}^{k-1}(max\{1-\mu_{\alpha_i}{}^{t},p\})}},\\ \sqrt[t]{\dfrac{\frac{\Pi_{i=1}^{k}(1-\mu^{t}_{\alpha_i})^{\vartheta_i}-\Pi_{i=1}^{k}(1-\mu^{t}{}_{\alpha_i}-\tau^{t}{}_{\alpha_i})^{\vartheta_i}}{\Pi_{i=1}^{k}(max\{1-\mu_{\alpha_i}{}^{t},p\})^{\vartheta_i-1}}}{\Pi_{i=1}^{k-1}(max\{1-\mu_{\alpha_i}{}^{t},p\})}}\end{array}\right)\oplus_{IDP}\left(\begin{array}{c}\sqrt[t]{1-\dfrac{\frac{(1-\mu_{\alpha_{k+1}}{}^{t})^{\vartheta_{k+1}}}{(max\{1-\mu_{\alpha_{k+1}}{}^{t},p\})^{\vartheta_{k+1}-1}}}{(max\{1-\mu_{\alpha_{k+1}}{}^{t},p\})}},\\ \sqrt[t]{\Pi_{i=1}^{k}\dfrac{\frac{(1-\mu^{t}{}_{\alpha_{k+1}})^{\vartheta_{k+1}}-(1-\mu^{t}{}_{\alpha_{k+1}}-\nu^{t}{}_{\alpha_{k+1}})^{\vartheta_{k+1}}}{(max\{1-\mu_{\alpha_{k+1}}{}^{t},p\})^{\vartheta_{k+1}-1}}}{(max\{1-\mu_{\alpha_{k+1}}{}^{t},p\})}},\\ \sqrt[t]{\Pi_{i=1}^{k}\dfrac{\frac{(1-\mu^{t}{}_{\alpha_{k+1}})^{\vartheta_{k+1}}-(1-\mu^{t}{}_{\alpha_{k+1}}-\tau^{t}{}_{\alpha_{k+1}})^{\vartheta_{k+1}}}{(max\{1-\mu_{\alpha_{k+1}}{}^{t},p\})^{\vartheta_{k+1}-1}}}{(max\{1-\mu_{\alpha_{k+1}}{}^{t},p\})}}\end{array}\right)\end{aligned}$$

$$=\left(\begin{array}{c}\sqrt[t]{1-\dfrac{\left(\frac{\Pi_{i=1}^{k}\frac{(1-\mu_{\alpha_i}{}^{t})^{\vartheta_i}}{(max\{1-\mu_{\alpha_i}{}^{t}\})^{\vartheta_i-1}}}{\Pi_{i=1}^{k-1}(max\{1-\mu_{\alpha_i}{}^{t},p\})}\right)\left(\frac{(1-\mu_{\alpha_{k+1}}{}^{t})^{\vartheta_{k+1}}}{(max\{1-\mu_{\alpha_{k+1}}{}^{t},p\})^{\vartheta_{k+1}-1}}\right)}{max\left\{\left(\frac{\Pi_{i=1}^{k}\frac{(1-\mu_{\alpha_i}{}^{t})^{\vartheta_i}}{(max\{1-\mu_{\alpha_i}{}^{t}\})^{\vartheta_i-1}}}{\Pi_{i=1}^{k-1}(max\{1-\mu_{\alpha_i}{}^{t},p\})}\right)\left(\frac{(1-\mu_{\alpha_{k+1}}{}^{t})^{\vartheta_{k+1}}}{(max\{1-\mu_{\alpha_{k+1}}{}^{t},p\})^{\vartheta_{k+1}-1}}\right),p\right\}}},\\ \sqrt[t]{\dfrac{\left(\frac{\Pi_{i=1}^{k}\frac{(1-\mu_{\alpha_i}{}^{t})^{\vartheta_i}}{(max\{1-\mu_{\alpha_i}{}^{t}\})^{\vartheta_i-1}}}{\Pi_{i=1}^{k-1}(max\{1-\mu_{\alpha_i}{}^{t},p\})}\right)\left(\frac{(1-\mu_{\alpha_{k+1}}{}^{t})^{\vartheta_{k+1}}}{(max\{1-\mu_{\alpha_{k+1}}{}^{t},p\})^{\vartheta_{k+1}-1}}\right)-\left(\left(\frac{\Pi_{i=1}^{k}\frac{(1-\mu_{\alpha_i}{}^{t}-\nu_{\alpha_i}{}^{t})^{\vartheta_i}}{\Pi_{i=1}^{k}(max\{1-\mu_{\alpha_i}{}^{t}\})^{\vartheta_i-1}}}{\Pi_{i=1}^{k-1}(max\{1-\mu_{\alpha_i}{}^{t},p\})}\right)\left(\frac{(1-\mu_{\alpha_{k+1}}{}^{t}-\nu_{\alpha_{k+1}}{}^{t})^{\vartheta_{k+1}}}{(max\{1-\mu_{\alpha_{k+1}}{}^{t},p\})^{\vartheta_{k+1}-1}}\right)\right)}{max\left\{\left(\frac{\Pi_{i=1}^{k}\frac{(1-\mu_{\alpha_i}{}^{t})^{\vartheta_i}}{(max\{1-\mu_{\alpha_i}{}^{t}\})^{\vartheta_i-1}}}{\Pi_{i=1}^{k-1}(max\{1-\mu_{\alpha_i}{}^{t},p\})}\right)\left(\frac{(1-\mu_{\alpha_{k+1}}{}^{t})^{\vartheta_{k+1}}}{(max\{1-\mu_{\alpha_{k+1}}{}^{t},p\})^{\vartheta_{k+1}-1}}\right),p\right\}}},\\ \sqrt[t]{\dfrac{\left(\frac{\Pi_{i=1}^{k}\frac{(1-\mu_{\alpha_i}{}^{t})^{\vartheta_i}}{(max\{1-\mu_{\alpha_i}{}^{t}\})^{\vartheta_i-1}}}{\Pi_{i=1}^{k-1}(max\{1-\mu_{\alpha_i}{}^{t},p\})}\right)\left(\frac{(1-\mu_{\alpha_{k+1}}{}^{t})^{\vartheta_{k+1}}}{(max\{1-\mu_{\alpha_{k+1}}{}^{t},p\})^{\vartheta_{k+1}-1}}\right)-\left(\left(\frac{\Pi_{i=1}^{k}\frac{(1-\mu_{\alpha_i}{}^{t}-\tau_{\alpha_i}{}^{t})^{\vartheta_i}}{\Pi_{i=1}^{k}(max\{1-\mu_{\alpha_i}{}^{t}\})^{\vartheta_i-1}}}{\Pi_{i=1}^{k-1}(max\{1-\mu_{\alpha_i}{}^{t},p\})}\right)\left(\frac{(1-\mu_{\alpha_{k+1}}{}^{t}-\tau_{\alpha_{k+1}}{}^{t})^{\vartheta_{k+1}}}{(max\{1-\mu_{\alpha_{k+1}}{}^{t},p\})^{\vartheta_{k+1}-1}}\right)\right)}{max\left\{\left(\frac{\Pi_{i=1}^{k}\frac{(1-\mu_{\alpha_i}{}^{t})^{\vartheta_i}}{(max\{1-\mu_{\alpha_i}{}^{t}\})^{\vartheta_i-1}}}{\Pi_{i=1}^{k-1}(max\{1-\mu_{\alpha_i}{}^{t},p\})}\right)\left(\frac{(1-\mu_{\alpha_{k+1}}{}^{t})^{\vartheta_{k+1}}}{(max\{1-\mu_{\alpha_{k+1}}{}^{t},p\})^{\vartheta_{k+1}-1}}\right),p\right\}}}\end{array}\right)$$

$$=\left(\begin{array}{c}\sqrt[t]{1-\dfrac{\Pi_{i=1}^{k+1}\frac{(1-\mu_{\alpha_i}{}^{t})^{\vartheta_i}}{(max\{1-\mu_{\alpha_i}{}^{t},p\})^{\vartheta_i-1}}}{\Pi_{i=1}^{k}(max\{1-\mu_{\alpha_i}{}^{t},p\})}},\\ \sqrt[t]{\dfrac{\frac{\Pi_{i=1}^{k+1}(1-\mu^{t}_{\alpha_i})^{\vartheta_i}-\Pi_{i=1}^{k+1}(1-\mu^{t}{}_{\alpha_i}-\nu^{t}{}_{\alpha_i})^{\vartheta_i}}{\Pi_{i=1}^{k+1}(max\{1-\mu_{\alpha_i}{}^{t},p\})^{\vartheta_i-1}}}{\Pi_{i=1}^{k}(max\{1-\mu_{\alpha_i}{}^{t},p\})}},\\ \sqrt[t]{\dfrac{\frac{\Pi_{i=1}^{k+1}(1-\mu^{t}_{\alpha_i})^{\vartheta_i}-\Pi_{i=1}^{k+1}(1-\mu^{t}{}_{\alpha_i}-\tau^{t}{}_{\alpha_i})^{\vartheta_i}}{\Pi_{i=1}^{k+1}(max\{1-\mu_{\alpha_i}{}^{t},p\})^{\vartheta_i-1}}}{\Pi_{i=1}^{k}(max\{1-\mu_{\alpha_i}{}^{t},p\})}}\end{array}\right)$$

Equation (4.12) is valid when n is replaced by $k+1$. Therefore, based on the principle of mathematical induction, Theorem 4.4 is established. □

Theorem 4.5. *Let $\kappa_i = \langle \mu_{\alpha_{\sigma_i}}, \nu_{\alpha_{\sigma_i}}, \tau_{\alpha_{\sigma_i}} \rangle$ be the collection of T-SPFNs, then T-SFIDPOWA is illustrated in Equation (4.13).*

$$T\text{-}SFIDPOWA(\kappa_1,\kappa_2,\ldots,\kappa_e)=\left(\begin{array}{c} \sqrt[t]{1-\dfrac{\Pi_{i=1}^{n}\frac{(1-\mu_{\alpha_{\sigma_i}}{}^{t})_i^{\vartheta}}{(max\{1-\mu_{\alpha_{\sigma_i}}{}^{t},p\})^{\vartheta_{\sigma_i}-1}}}{\Pi_{i=1}^{n-1}(max\{1-\mu_{\alpha_{\sigma_i}}{}^{t},p\})}}, \\ \sqrt[t]{\dfrac{\frac{\Pi_{i=1}^{n}(1-\mu^{t}{}_{\alpha_{\sigma_i}})_i^{\vartheta}-\Pi_{i=1}^{n}(1-\mu^{t}{}_{\alpha_{\sigma_i}}-\nu^{t}{}_{\alpha_{\sigma_i}})_i^{\vartheta}}{\Pi_{i=1}^{n}(max\{1-\mu_{\alpha_{\sigma_i}}{}^{t},p\})^{\vartheta_{\sigma_i}-1}}}{\Pi_{i=1}^{n-1}(max\{1-\mu_{\alpha_{\sigma_i}}{}^{t},p\})}}, \\ \sqrt[t]{\dfrac{\frac{\Pi_{i=1}^{n}(1-\mu^{t}{}_{\alpha_{\sigma_i}})_i^{\vartheta}-\Pi_{i=1}^{n}(1-\mu^{t}{}_{\alpha_{\sigma_i}}-\tau^{t}{}_{\alpha_{\sigma_i}})^{\vartheta_{\sigma_{\sigma_i}}}}{\Pi_{i=1}^{n}(max\{1-\mu_{\alpha_{\sigma_i}}{}^{t},p\})^{\vartheta_i-1}}}{\Pi_{i=1}^{n-1}(max\{1-\mu_{\alpha_{\sigma_i}}{}^{t},p\})}} \end{array}\right) \tag{4.13}$$

where ϑ_i is the WV of $\kappa_{(i)}$ with $\vartheta_i > 0$ and $\sum_{i=1}^{e} \vartheta_i = 1$.

Proof. It is easy to prove. □

It can be established that the T-SFIDPWA operator possesses several fundamental properties, including idempotency, permutation invariance, monotonicity, and boundedness. A detailed exposition of these properties is available within this paper; however, for the sake of conciseness, we omit the proofs here. The T-SPFIDP operations, as outlined in Equations (4.1) through (4.4), serve as the foundation for these properties.

Theorem 4.6. *(Idempotency) Let $\kappa_i = \langle \mu_i, \nu_i, \tau_i \rangle$ be the collection of T-SPFNs and $\kappa_\diamond = \langle \mu_\diamond, \nu_\diamond, \tau_\diamond \rangle$ be the T-SPFNs such that, $\kappa_i = \kappa_\diamond \forall i$. Then Idempotency shows in Equation (4.14).*

$$T\text{-}SFIDPWA(\kappa_1,\kappa_2,\ldots,\kappa_e) = \kappa_\diamond \tag{4.14}$$

Theorem 4.7. *(Boundedness) Let $\kappa_i = \langle \mu_i, \nu_i, \tau_i \rangle$ be the collection of T-SPFNs. Then for $T\text{-}SFIDPWA(\kappa_1,\kappa_2,\ldots,\kappa_e) = \langle \mu_x, \nu_x, \tau_x \rangle$. Then Boundedness shows in Equation (4.15).*

$$\min_i \left\{\mu^t{}_i + \nu^t + \tau^t{}_i\right\} \le \mu^t{}_x + \nu^t{}_x + \tau^t{}_x \le \max_i \left\{\mu^t{}_i + \nu^t{}_i + \tau^t{}_i\right\} \tag{4.15}$$

Theorem 4.8. *(Monotonicity) Assume that $\kappa_i = \langle \mu_i, \nu_i, \tau_i \rangle$ and $\kappa_{i^*} = \langle \mu_{i^*}, \nu_{i^*}, \tau_{i^*} \rangle$ are the families of T-SPFNs, and also consider*

$$T\text{-}SFIDPWA(\kappa_1,\kappa_2,\ldots\kappa_e) \;=\; \kappa \;=\; \langle \mu, \nu, \tau \rangle$$

and

$$T\text{-}SFIDPWA(\kappa_{1*},\kappa_{2*},\ldots\kappa_{e^*}) \;=\; \kappa_* \;=\; \langle \mu_*, \nu_*, \tau_* \rangle.$$

Then Monotonicity shows in Equation (4.16).

$$\mu^t + \nu^t + \tau^t \le \mu^t{}_* + \nu^t{}_* + \tau^t{}_*, \quad if \quad \mu^t{}_i + \nu^t{}_i + \tau^t{}_i \le \mu^t{}_{i^*} + \nu^t{}_{i^*} + \tau^t{}_{i^*} \tag{4.16}$$

Theorem 4.9. *(Permutation invariance) Assume that $\kappa_i = \langle \mu_i, \nu_i, \tau_i \rangle$ is the replacement of the $\kappa_{i^*} = \langle \mu_{i^*}, \nu_{i^*}, \tau_{i^*} \rangle$. Then, the T-SFIDPWA operator satisfies permutation invariance as shown in Equation (4.17).*

$$T\text{-}SFIDPWA(\langle \mu_i, \nu_i, \tau_i \rangle) = T\text{-}SFIDPWA(\langle \mu_{i^*}, \nu_{i^*}, \tau_{i^*} \rangle) \tag{4.17}$$

4.2. T-SFIDPWG operators

Definition 4.10. Let $\kappa_i = \langle \mu_{\alpha_{(i)}}, \nu_{\alpha_{(i)}}, \tau_{\alpha_{(i)}} \rangle$ be the collection of T-SPFNs, and T-SFIDPWG: $\mathrm{R}^n \to \mathrm{R}$, be the mapping as shown in Equation (4.18).

$$\text{T-SFIDPWG}(\kappa_1,\kappa_2,\ldots\kappa_e) = \left(\vartheta_1 * \kappa_1 \tilde{\oplus}_{IDP} \vartheta_2 * \kappa_2 \tilde{\oplus}_{IDP} \ldots, \tilde{\oplus}_{IDP} \vartheta_e * \kappa_e\right) \tag{4.18}$$

then the mapping T-SFIDPWG is called “T-spherical fuzzy interactive Dubois–Prade weighted geometric (T-SFIDPWG) operator”, here $w = (\vartheta_1, \ldots, \vartheta_e)$ is the weight vector (WV) of $\kappa_{(i)}$ with $\vartheta_i > 0$ and $\sum_{i=1}^{e} \vartheta_i = 1$.

We may also investigate T-SFIDPWG using proposed operational rules, as demonstrated in the theorem.

Theorem 4.11. *Let $\kappa_i = \langle \mu_{\alpha_i}, \nu_{\alpha_i}, \tau_{\alpha_i} \rangle$ be the collection of T-SPFNs. Then T-SFIDPWG is shown in Equation (4.19).*

$$\text{T-SFIDPWG}(\kappa_1,\kappa_2,\ldots,\kappa_e)=\begin{pmatrix} \sqrt[t]{\dfrac{\frac{\Pi_{i=1}^{n}(1-\nu^{t}_{\alpha_i})^{\vartheta_i}-\Pi_{i=1}^{n}(1-\nu^{t}{\alpha_i}-\mu^{t}{\alpha_i})^{\vartheta_i}}{\Pi_{i=1}^{n}(max\{1-\nu_{\alpha_i}{}^{t},p\})^{\vartheta_i-1}}}{\Pi_{i=1}^{n-1}(max\{1-\nu_{\alpha_i}{}^{t},p\})}}, \\ \sqrt[t]{1-\dfrac{\Pi_{i=1}^{n}\frac{(1-\nu_{\alpha_i}{}^{t})^{\vartheta_i}}{(max\{1-\nu_{\alpha_i}{}^{t},p\})^{\vartheta_i-1}}}{\Pi_{i=1}^{n-1}(max\{1-\nu_{\alpha_i}{}^{t},p\})}}, \\ \sqrt[t]{\dfrac{\frac{\Pi_{i=1}^{n}(1-\nu^{t}_{\alpha_i})^{\vartheta_i}-\Pi_{i=1}^{n}(1-\nu^{t}{\alpha_i}-\tau^{t}{\alpha_i})^{\vartheta_i}}{\Pi_{i=1}^{n}(max\{1-\nu_{\alpha_i}{}^{t},p\})^{\vartheta_i-1}}}{\Pi_{i=1}^{n-1}(max\{1-\nu_{\alpha_i}{}^{t},p\})}} \end{pmatrix} \tag{4.19}$$

where ϑ_i is the WV of $\kappa_{(i)}$ with $\vartheta_i > 0$ and $\sum_{i=1}^{e}\vartheta_i = 1$.

Proof. Theorem 4.11 can be proven by mathematical induction.
for $n = 2$ we have

$$\vartheta_1^{\gamma} * \kappa_2 = \begin{pmatrix} \sqrt[t]{\left(\dfrac{(1-\nu^{t}{\alpha_1})^{\vartheta_1}-(1-\nu^{t}{\alpha_1}-\mu^{t}{\alpha_1})}{(max\{1-\nu^{t}{\alpha_1},p\})^{\vartheta_1-1}}\right)}, \\ \sqrt[t]{\left(1-\dfrac{(1-\nu^{t}{\alpha_1})^{\vartheta_1}}{(max\{1-\nu^{t}{\alpha_1},p\})^{\vartheta_1-1}}\right)}, \\ \sqrt[t]{\left(\dfrac{(1-\nu^{t}{\alpha_1})^{\vartheta_1}-(1-\nu^{t}{\alpha_1}-\tau^{t}{\alpha_1})}{(max\{1-\nu^{t}{\alpha_1},p\})^{\vartheta_i-1}}\right)} \end{pmatrix}$$

$$\vartheta_2^{\gamma} * \kappa_2 = \begin{pmatrix} \sqrt[t]{\left(\dfrac{(1-\nu^{t}{\alpha_2})^{\vartheta_2}-(1-\nu^{t}{\alpha_2}-\mu^{t}{\alpha_2})}{(max\{1-\nu^{t}{\alpha_2},p\})^{\vartheta_2-1}}\right)}, \\ \sqrt[t]{\left(1-\dfrac{(1-\nu^{t}{\alpha_2})^{\vartheta_2}}{(max\{1-\nu^{t}{\alpha_2},p\})^{\vartheta_2-1}}\right)}, \\ \sqrt[t]{\left(\dfrac{(1-\nu^{t}{\alpha_2})^{\vartheta_2}-(1-\nu^{t}{\alpha_2}-\tau^{t}{\alpha_2})}{(max\{1-\nu^{t}{\alpha_2},p\})^{\vartheta_2-1}}\right)} \end{pmatrix}$$

$$\text{T-SFIDPWG}(\kappa_1,\kappa_2) = \begin{pmatrix} \sqrt[t]{\left(\dfrac{\left(\frac{(1-\nu^{t}{\alpha_1})^{\vartheta_1}}{(max\{1-\nu^{t}{\alpha_1},p\})^{\vartheta_1-1}}\right)\left(\frac{(1-\nu^{t}{\alpha_2})^{\vartheta_2}}{(max\{1-\nu^{t}{\alpha_2},p\})^{\vartheta_2-1}}\right)-\left(\frac{(1-\nu^{t}{\alpha_1}-\mu_{\alpha_1})^{\vartheta_2}}{(max\{1-\nu^{t}{\alpha_1},p\})^{\vartheta_1-1}}\right)\left(\frac{(1-\nu^{t}{\alpha_2}-\mu_{\alpha_2})^{\vartheta_2}}{(max\{1-\nu^{t}{\alpha_2},p\})^{\vartheta_2-1}}\right)}{max\left\{\left(\frac{(1-\nu^{t}{\alpha_1})^{\vartheta_1}}{(max\{1-\nu^{t}{\alpha_1},p\})^{\vartheta_1-1}}\right)\left(\frac{(1-\nu^{t}{\alpha_2})^{\vartheta_1}}{(max\{1-\nu^{t}{\alpha_2},p\})^{\vartheta_2-1}}\right),p\right\}}\right)}, \\ \sqrt[t]{\left(1-\dfrac{\left(\frac{(1-\nu^{t}{\alpha_1})^{\vartheta_1}}{(max\{1-\nu^{t}{\alpha_1},p\})^{\vartheta_1-1}}\right)\left(\frac{(1-\nu^{t}{\alpha_2})^{\vartheta_2}}{(max\{1-\nu^{t}{\alpha_2},p\})^{\vartheta_2-1}}\right)}{max\left\{\left(\frac{(1-\nu^{t}{\alpha_1})^{\vartheta_1}}{(max\{1-\nu^{t}{\alpha_1},p\})^{\vartheta_1-1}}\right)\left(\frac{(1-\nu^{t}{\alpha_2})^{\vartheta_2}}{(max\{1-\nu^{t}{\alpha_2},p\})^{\vartheta_2-1}}\right),p\right\}}\right)}, \\ \sqrt[t]{\left(\dfrac{\left(\frac{(1-\nu^{t}{\alpha_1})^{\vartheta_1}}{(max\{1-\nu^{t}{\alpha_1},p\})^{\vartheta_1-1}}\right)\left(\frac{(1-\nu^{t}{\alpha_2})^{\vartheta_2}}{(max\{1-\nu^{t}{\alpha_2},p\})^{\vartheta_2-1}}\right)-\left(\frac{(1-\nu^{t}{\alpha_1}-\tau_{\alpha_1})^{\vartheta_1}}{(max\{1-\nu^{t}{\alpha_1},p\})^{\vartheta_1-1}}\right)\left(\frac{(1-\nu^{t}{\alpha_2}-\tau_{\alpha_2})^{\vartheta_2}}{(max\{1-\nu^{t}{\alpha_2},p\})^{\vartheta_2-1}}\right)}{max\left\{\left(\frac{(1-\nu^{t}{\alpha_1})^{\vartheta_1}}{(max\{1-\nu^{t}{\alpha_1},p\})^{\vartheta_1-1}}\right)\left(\frac{(1-\nu^{t}{\alpha_2})^{\vartheta_2}}{(max\{1-\nu^{t}{\alpha_2},p\})^{\vartheta_2-1}}\right),p\right\}}\right)} \end{pmatrix}$$

$$= \begin{pmatrix} \sqrt[t]{\dfrac{\frac{\Pi_{i=1}^{2}(1-\nu^{t}_{\alpha_i})^{\vartheta_i}-\Pi_{i=1}^{2}(1-\nu^{t}{\alpha_i}-\mu^{t}{\alpha_i})^{\vartheta_i}}{\Pi_{i=1}^{2}(max\{1-\nu_{\alpha_i}{}^{t},p\})^{\vartheta_i-1}}}{(max\{1-\nu_{\alpha_i}{}^{t},p\})}}, \\ \sqrt[t]{1-\dfrac{\Pi_{i=1}^{2}\frac{(1-\nu_{\alpha_i}{}^{t})^{\vartheta_i}}{(max\{1-\nu_{\alpha_i}{}^{t},p\})^{\vartheta_i-1}}}{\Pi_{i=1}^{2-1}(max\{1-\nu_{\alpha_i}{}^{t},p\})}}, \\ \sqrt[t]{\dfrac{\frac{\Pi_{i=1}^{2}(1-\nu^{t}_{\alpha_i})^{\vartheta_i}-\Pi_{i=1}^{2}(1-\nu^{t}{\alpha_i}-\tau^{t}{\alpha_i})^{\vartheta_i}}{\Pi_{i=1}^{2}(max\{1-\nu_{\alpha_i}{}^{t},p\})^{\vartheta_i-1}}}{(max\{1-\nu_{\alpha_i}{}^{t},p\})}} \end{pmatrix}$$

This shows that Equation 4.11 hold for $n = 2$ and assuming that Equation 4.11 hold for $n = k$, then we have

$$\text{T-SFIDPWG}(\kappa_1,\kappa_2,\dots,\kappa_k)=\left(\begin{array}{c}\sqrt[t]{\dfrac{\dfrac{\prod_{i=1}^{k}(1-v^{t}_{\alpha_i})^{\vartheta_i}-\prod_{i=1}^{k}(1-v^{t}{\alpha_i}-\mu^{t}{\alpha_i})^{\vartheta_i}}{\prod_{i=1}^{k}(max\{1-v_{\alpha_i}{}^{t},p\})^{\vartheta_i-1}}}{\prod_{i=1}^{k-1}(max\{1-v_{\alpha_i}{}^{t},p\})}},\\ \sqrt[t]{1-\dfrac{\prod_{i=1}^{k}\dfrac{(1-v_{\alpha_i}{}^{t})^{\vartheta_i}}{(max\{1-v_{\alpha_i}{}^{t},p\})^{\vartheta_i-1}}}{\prod_{i=1}^{k-1}(max\{1-v_{\alpha_i}{}^{t},p\})}},\\ \sqrt[t]{\dfrac{\dfrac{\prod_{i=1}^{k}(1-v^{t}_{\alpha_i})^{\vartheta_i}-\prod_{i=1}^{k}(1-v^{t}{\alpha_i}-\tau^{t}{\alpha_i})^{\vartheta_i}}{\prod_{i=1}^{k}(max\{1-v_{\alpha_i}{}^{t},p\})^{\vartheta_i-1}}}{\prod_{i=1}^{k-1}(max\{1-v_{\alpha_i}{}^{t},p\})}}\end{array}\right)$$

When $n = k + 1$, we have

$$\begin{aligned}&\text{T-SFIDPWG}(\kappa_1,\kappa_2,\dots,\kappa_k,\kappa_{k+1})\\ &=\left(\begin{array}{c}\sqrt[t]{\dfrac{\dfrac{\prod_{i=1}^{k}(1-v^{t}_{\alpha_i})^{\vartheta_i}-\prod_{i=1}^{k}(1-v^{t}{\alpha_i}-\mu^{t}{\alpha_i})^{\vartheta_i}}{\prod_{i=1}^{k}(max\{1-v_{\alpha_i}{}^{t},p\})^{\vartheta_i-1}}}{\prod_{i=1}^{k-1}(max\{1-v_{\alpha_i}{}^{t},p\})}},\\ \sqrt[t]{1-\dfrac{\prod_{i=1}^{k}\dfrac{(1-v_{\alpha_i}{}^{t})^{\vartheta_i}}{(max\{1-v_{\alpha_i}{}^{t},p\})^{\vartheta_i-1}}}{\prod_{i=1}^{k-1}(max\{1-v_{\alpha_i}{}^{t},p\})}},\\ \sqrt[t]{\dfrac{\dfrac{\prod_{i=1}^{k}(1-v^{t}_{\alpha_i})^{\vartheta_i}-\prod_{i=1}^{k}(1-v^{t}{\alpha_i}-\tau^{t}{\alpha_i})^{\vartheta_i}}{\prod_{i=1}^{k}(max\{1-v_{\alpha_i}{}^{t},p\})^{\vartheta_i-1}}}{\prod_{i=1}^{k-1}(max\{1-v_{\alpha_i}{}^{t},p\})}}\end{array}\right)\oplus_{IDP}\left(\begin{array}{c}\sqrt[t]{\prod_{i=1}^{k}\dfrac{\dfrac{(1-v^{t}{\alpha_{k+1}})^{\vartheta_{k+1}}-(1-v^{t}{\alpha_{k+1}}-\mu^{t}{\alpha_{k+1}})^{\vartheta_{k+1}}}{(max\{1-v_{\alpha_{k+1}}{}^{t},p\})^{\vartheta_{k+1}-1}}}{(max\{1-v_{\alpha_{k+1}}{}^{t},p\})}},\\ \sqrt[t]{1-\dfrac{\dfrac{(1-v_{\alpha_{k+1}}{}^{t})^{\vartheta_{k+1}}}{(max\{1-v_{\alpha_{k+1}}{}^{t},p\})^{\vartheta_{k+1}-1}}}{(max\{1-v_{\alpha_{k+1}}{}^{t},p\})}},\\ \sqrt[t]{\prod_{i=1}^{k}\dfrac{\dfrac{(1-v^{t}{\alpha_{k+1}})^{\vartheta_{k+1}}-(1-v^{t}{\alpha_{k+1}}-\tau^{t}{\alpha_{k+1}})^{\vartheta_{k+1}}}{(max\{1-v_{\alpha_{k+1}}{}^{t},p\})^{\vartheta_{k+1}-1}}}{(max\{1-v_{\alpha_{k+1}}{}^{t},p\})}}\end{array}\right)\end{aligned}$$

$$=\left(\begin{array}{c}\sqrt[t]{\dfrac{\left(\dfrac{\prod_{i=1}^{k}\dfrac{(1-v_{\alpha_i}{}^{t})^{\vartheta_i}}{(max\{1-v_{\alpha_i}{}^{t}\})^{\vartheta_i-1}}}{\prod_{i=1}^{k-1}(max\{1-v_{\alpha_i}{}^{t},p\})}\right)\left(\dfrac{(1-v_{\alpha_{k+1}}{}^{t})^{\vartheta_{k+1}}}{(max\{1-v_{\alpha_{k+1}}{}^{t},p\})^{\vartheta_{k+1}-1}}\right)-\left(\left(\dfrac{\dfrac{\prod_{i=1}^{k}(1-v_{\alpha_i}{}^{t}-\mu_{\alpha_i}{}^{t})^{\vartheta_i}}{\prod_{i=1}^{k}(max\{1-v_{\alpha_i}{}^{t}\})^{\vartheta_i-1}}}{\prod_{i=1}^{k-1}(max\{1-v_{\alpha_i}{}^{t},p\})}\right)\left(\dfrac{(1-v_{\alpha_{k+1}}{}^{t}-\mu_{\alpha_{k+1}}{}^{t})^{\vartheta_{k+1}}}{(max\{1-v_{\alpha_{k+1}}{}^{t},p\})^{\vartheta_{k+1}-1}}\right)\right)}{max\left\{\left(\dfrac{\prod_{i=1}^{k}\dfrac{(1-v_{\alpha_i}{}^{t})^{\vartheta_i}}{(max\{1-v_{\alpha_i}{}^{t}\})^{\vartheta_i-1}}}{\prod_{i=1}^{k-1}(max\{1-v_{\alpha_i}{}^{t},p\})}\right)\left(\dfrac{(1-v_{\alpha_{k+1}}{}^{t})^{\vartheta_{k+1}}}{(max\{1-v_{\alpha_{k+1}}{}^{t},p\})^{\vartheta_{k+1}-1}}\right),p\right\}}},\\ \sqrt[t]{1-\dfrac{\left(\dfrac{\prod_{i=1}^{k}\dfrac{(1-v_{\alpha_i}{}^{t})^{\vartheta_i}}{(max\{1-v_{\alpha_i}{}^{t}\})^{\vartheta_i-1}}}{\prod_{i=1}^{k-1}(max\{1-v_{\alpha_i}{}^{t},p\})}\right)\left(\dfrac{(1-v_{\alpha_{k+1}}{}^{t})^{\vartheta_{k+1}}}{(max\{1-v_{\alpha_{k+1}}{}^{t},p\})^{\vartheta_{k+1}-1}}\right)}{max\left\{\left(\dfrac{\prod_{i=1}^{k}\dfrac{(1-v_{\alpha_i}{}^{t})^{\vartheta_i}}{(max\{1-v_{\alpha_i}{}^{t}\})^{\vartheta_i-1}}}{\prod_{i=1}^{k-1}(max\{1-v_{\alpha_i}{}^{t},p\})}\right)\left(\dfrac{(1-v_{\alpha_{k+1}}{}^{t})^{\vartheta_{k+1}}}{(max\{1-v_{\alpha_{k+1}}{}^{t},p\})^{\vartheta_{k+1}-1}}\right),p\right\}}},\\ \sqrt[t]{\dfrac{\left(\dfrac{\prod_{i=1}^{k}\dfrac{(1-v_{\alpha_i}{}^{t})^{\vartheta_i}}{(max\{1-v_{\alpha_i}{}^{t}\})^{\vartheta_i-1}}}{\prod_{i=1}^{k-1}(max\{1-v_{\alpha_i}{}^{t},p\})}\right)\left(\dfrac{(1-v_{\alpha_{k+1}}{}^{t})^{\vartheta_{k+1}}}{(max\{1-v_{\alpha_{k+1}}{}^{t},p\})^{\vartheta_{k+1}-1}}\right)-\left(\left(\dfrac{\dfrac{\prod_{i=1}^{k}(1-v_{\alpha_i}{}^{t}-\tau_{\alpha_i}{}^{t})^{\vartheta_i}}{\prod_{i=1}^{k}(max\{1-v_{\alpha_i}{}^{t}\})^{\vartheta_i-1}}}{\prod_{i=1}^{k-1}(max\{1-v_{\alpha_i}{}^{t},p\})}\right)\left(\dfrac{(1-v_{\alpha_{k+1}}{}^{t}-\tau_{\alpha_{k+1}}{}^{t})^{\vartheta_{k+1}}}{(max\{1-v_{\alpha_{k+1}}{}^{t},p\})^{\vartheta_{k+1}-1}}\right)\right)}{max\left\{\left(\dfrac{\prod_{i=1}^{k}\dfrac{(1-v_{\alpha_i}{}^{t})^{\vartheta_i}}{(max\{1-v_{\alpha_i}{}^{t}\})^{\vartheta_i-1}}}{\prod_{i=1}^{k-1}(max\{1-v_{\alpha_i}{}^{t},p\})}\right)\left(\dfrac{(1-v_{\alpha_{k+1}}{}^{t})^{\vartheta_{k+1}}}{(max\{1-v_{\alpha_{k+1}}{}^{t},p\})^{\vartheta_{k+1}-1}}\right),p\right\}}}\end{array}\right)$$

$$=\left(\begin{array}{c}\sqrt[t]{\dfrac{\dfrac{\prod_{i=1}^{k+1}(1-v^{t}_{\alpha_i})^{\vartheta_i}-\prod_{i=1}^{k+1}(1-v^{t}{\alpha_i}-\mu^{t}{\alpha_i})^{\vartheta_i}}{\prod_{i=1}^{k+1}(max\{1-v_{\alpha_i}{}^{t},p\})^{\vartheta_i-1}}}{\prod_{i=1}^{k}(max\{1-v_{\alpha_i}{}^{t},p\})}},\\ \sqrt[t]{1-\dfrac{\prod_{i=1}^{k+1}\dfrac{(1-v_{\alpha_i}{}^{t})^{\vartheta_i}}{(max\{1-v_{\alpha_i}{}^{t},p\})^{\vartheta_i-1}}}{\prod_{i=1}^{k}(max\{1-v_{\alpha_i}{}^{t},p\})}},\\ \sqrt[t]{\dfrac{\dfrac{\prod_{i=1}^{k+1}(1-v^{t}_{\alpha_i})^{\vartheta_i}-\prod_{i=1}^{k+1}(1-v^{t}{\alpha_i}-\tau^{t}{\alpha_i})^{\vartheta_i}}{\prod_{i=1}^{k+1}(max\{1-v_{\alpha_i}{}^{t},p\})^{\vartheta_i-1}}}{\prod_{i=1}^{k}(max\{1-v_{\alpha_i}{}^{t},p\})}}\end{array}\right)$$

Equation (5.2) is valid when n is replaced by $k+1$. Therefore, based on the principle of mathematical induction, Theorem 4.11 is confirmed. □

Theorem 4.12. *Let $\kappa_i = \langle \mu_{\alpha_{\sigma_i}}, \nu_{\alpha_{\sigma_i}}, \tau_{\alpha_{\sigma_i}} \rangle$ be the collection of T-SPFNs, we can also find T-spherical fuzzy interactive Dubois–Prade order weighted geometric (T-SFIDPOWG) by Equation (4.20).*

$$T\text{-}SFIDPOWG(\kappa_1, \kappa_2, \ldots, \kappa_e) = \left(\begin{array}{c} \sqrt[t]{\dfrac{\dfrac{\Pi_{i=1}^{n}(1-\nu^t{}_{\alpha_{\sigma_i}})_i^{\vartheta} - \Pi_{i=1}^{n}(1-\nu^t{}_{\alpha_{\sigma_i}} - \mu^t{}_{\alpha_{\sigma_i}})_i^{\vartheta}}{\Pi_{i=1}^{n}(max\{1-\nu_{\alpha_{\sigma_i}}{}^t, p\})^{\vartheta_{\sigma_i}-1}}}{\Pi_{i=1}^{n-1}(max\{1-\nu_{\alpha_{\sigma_i}}{}^t, p\})}}, \\ \sqrt[t]{1 - \dfrac{\Pi_{i=1}^{n}\dfrac{(1-\nu_{\alpha_{\sigma_i}}{}^t)_i^{\vartheta}}{(max\{1-\nu_{\alpha_{\sigma_i}}{}^t, p\})^{\vartheta_{\sigma_i}-1}}}{\Pi_{i=1}^{n-1}(max\{1-\nu_{\alpha_{\sigma_i}}{}^t, p\})}}, \\ \sqrt[t]{\dfrac{\dfrac{\Pi_{i=1}^{n}(1-\nu^t{}_{\alpha_{\sigma_i}})_i^{\vartheta} - \Pi_{i=1}^{n}(1-\nu^t{}_{\alpha_{\sigma_i}} - \tau^t{}_{\alpha_{\sigma_i}})^{\vartheta_{\sigma_{\sigma_i}}}}{\Pi_{i=1}^{n}(max\{1-\nu_{\alpha_{\sigma_i}}{}^t, p\})^{\vartheta_i-1}}}{\Pi_{i=1}^{n-1}(max\{1-\nu_{\alpha_{\sigma_i}}{}^t, p\})}} \end{array} \right) \tag{4.20}$$

where ϑ_i is the WV of $\kappa_{(i)}$ with $\vartheta_i > 0$ and $\sum_{i=1}^{e} \vartheta_i = 1$.

Proof. It is easy to prove. □

It can be established that the T-SFIDPWG operator possesses several fundamental properties, including idempotency, permutation invariance, monotonicity, and boundedness. A detailed exposition of these properties is available within this paper; however, for the sake of conciseness, we omit the proofs here. The T-SPFIDP operations, as outlined in Equations (4.1) - (4.4), serve as the foundation for these properties.

Theorem 4.13. *(Idempotency) Let $\kappa_i = \langle \mu_i, \nu_i, \tau_i \rangle$ be the collection of T-SPFNs and $\kappa_\diamond = \langle \mu_\diamond, \nu_\diamond, \tau_\diamond \rangle$ be the T-SPFNs such that, $\kappa_i = \kappa_\diamond \forall i$. The Idempotency is shown in Equation (4.21).*

$$T\text{-}SFIDPWG(\kappa_1, \kappa_2, \ldots, \kappa_e) = \kappa_\diamond \tag{4.21}$$

Theorem 4.14. *(Boundedness) Let $\kappa_i = \langle \mu_i, \nu_i, \tau_i \rangle$ be the collection of T-SPFNs. Then for $T\text{-}SFIDPWG(\kappa_1, \kappa_2, \ldots, \kappa_e) = \langle \mu_x, \nu_x, \tau_x \rangle$. The Boundedness is shown in Equation (4.22).*

$$\min_i \left\{ \mu^t{}_i + \nu^t + \tau^t{}_i \right\} \leq \mu^t{}_x + \nu^t{}_x + \tau^t{}_x \leq \max_i \left\{ \mu^t{}_i + \nu^t{}_i + \tau^t{}_i \right\} \tag{4.22}$$

Theorem 4.15. *(Monotonicity) Assume that $\kappa_i = \langle \mu_i, \nu_i, \tau_i \rangle$ and $\kappa_{i^*} = \langle \mu_{i^*}, \nu_{i^*}, \tau_{i^*} \rangle$ are the families of T-SPFNs. The Monotonicity is shown in Equation (4.23).*

$$T\text{-}SFIDPWG(\kappa_1, \kappa_2, \ldots \kappa_e) = \kappa = \langle \mu, \nu, \tau \rangle$$

and

$$T\text{-}SFIDPWG(\kappa_{1^*}, \kappa_{2^*}, \ldots \kappa_{e^*}) = \kappa_* = \langle \mu_*, \nu_*, \tau_* \rangle.$$

Then,

$$\mu^t + \nu^t + \tau^t \leq \mu^t{}_* + \nu^t{}_* + \tau^t{}_*, \quad \text{if} \quad \mu^t{}_i + \nu^t{}_i + \tau^t{}_i \leq \mu^t{}_{i^*} + \nu^t{}_{i^*} + \tau^t{}_{i^*} \tag{4.23}$$

Theorem 4.16. *(Permutation invariance) Assume that $\kappa_i = \langle \mu_i, \nu_i, \tau_i \rangle$ is the replacement of the $\kappa_{i^*} = \langle \mu_{i^*}, \nu_{i^*}, \tau_{i^*} \rangle$. Then, the T-SFIDPWG operator satisfies permutation invariance shown in Equation (4.24).*

$$T\text{-}SFIDPWG(\langle \mu_i, \nu_i, \tau_i \rangle) = T\text{-}SFIDPWG(\langle \mu_{i^*}, \nu_{i^*}, \tau_{i^*} \rangle) \tag{4.24}$$

5. Algorithm

Step 1: Input the T-SPFNs data set of against the suitable alternatives $\mathrm{A_k}; (k = 1, 2, \ldots, m)$ and under the effect of various criteria $\mathrm{Cri_p}; (p = 1, 2, \ldots, n)$

Table 2
Linguistic terms for evaluation.

Evaluation Term	Description	T-SPFNs
1. Exceptionally Efficient (EE)	Exceptional cost-efficiency, low investment, and operational costs.	$\langle 0.90, 0.05, 0.10\rangle$
2. Highly Trustworthy (HT)	Outstanding reliability, flexibility, and supply security.	$\langle 0.85, 0.10, 0.15\rangle$
3. Positively Impactful (PI)	Strong positive impact on economic development, low carbon emissions, and waste disposal.	$\langle 0.80, 0.20, 0.25\rangle$
4. Moderately Effective (ME)	Decent cost-efficiency and operational effectiveness.	$\langle 0.75, 0.20, 0.30\rangle$
5. Acceptable (A)	Meets basic requirements without significant advantages or disadvantages.	$\langle 0.60, 0.30, 0.45\rangle$
6. Marginally Satisfactory (MS)	Some positive aspects but also significant drawbacks or uncertainties.	$\langle 0.55, 0.35, 0.50\rangle$
7. Inappropriate (I)	Moderate level of cost-effectiveness and operational efficiency.	$\langle 0.30, 0.40, 0.70\rangle$
8. Highly Inappropriate (IH)	Costly, unreliable, and adverse effects on economic and environmental factors.	$\langle 0.20, 0.40, 0.80\rangle$

Table 3
Decision-Makers in power system reforms.

Decision-Maker	Role	Key Decisions/Responsibilities
1. Government Authorities	Policymakers initiating and implementing reforms.	Decisions on market structure, privatization, regulations, and energy policy.
(0.90, 0.20, 0.10)	(0.80, 0.15, 0.20)	(0.85, 0.20, 0.20)
2. Regulatory Bodies	Oversee rules and bridge between government and industry.	Decide tariffs, and market rules, and ensure fair competition.
(0.80, 0.25, 0.30)	(0.70, 0.20, 0.40)	(0.75, 0.35, 0.40)
3. Utility Companies	Implement reforms, and adapt to new tech.	Decide on investments, technology adoption, and operational efficiency.
(0.60, 0.40, 0.55)	(0.65, 0.35, 0.50)	(0.60, 0.40, 0.55)

Decision-makers enter the decision matrices $\mathrm{C} = \left[\mathrm{C_{ij}}\right]_{n\times m}$

$$
\begin{array}{c c}
 & \begin{array}{cccc} \mathrm{C}_1 & \mathrm{C}_2 & & \mathrm{C_m} \end{array} \\
\begin{array}{c} \mathrm{A}_1 \\ \mathrm{A}_2 \\ \vdots \\ \mathrm{A_n} \end{array} &
\begin{bmatrix}
(\Upsilon_{11}, \Upsilon_{11}, \Upsilon_{11}) & (\Upsilon_{12}, \Upsilon_{12}, \Upsilon_{12},) & \dots & (\Upsilon_{1m}, \Upsilon_{1m}, \Upsilon_{1m}) \\
(\Upsilon_{21}, \Upsilon_{21}, \Upsilon_{21}) & (\Upsilon_{22}, \Upsilon_{22}, \Upsilon_{22}) & \dots & (\Upsilon_{2m}, \Upsilon_{2m}, \Upsilon_{2m}) \\
\vdots & \vdots & \ddots & \vdots \\
(\Upsilon_{n1}, \Upsilon_{n1}, \Upsilon_{n1},) & (\Upsilon_{n2}, \Upsilon_{n2}, \Upsilon_{n2}) & \dots & (\Upsilon_{nm}, \Upsilon_{nm}, \Upsilon_{nm})
\end{bmatrix}
\end{array}
$$

Where $\mathrm{C^l_{ij}} = \left(\Upsilon_{ij}, \Upsilon_{ij}, \Upsilon_{ij}\right)$ where (i = 1,2,...,n) and (j = 1,2,...,m) is the T-SPFNs information, representing the corresponding alternatives under the decision-maker criteria. The eight linguistic terms assigned to criteria against each alternative, as elucidated in Table 2, are complemented by the linguistic terms associated with expertise specified in Table 3. This comprehensive set of linguistic terms facilitates a thorough evaluation.

Step 2: Calculate the weights of decision-makers by employing a score function given in Equation (2.2). Afterward, utilize these calculated scores in the specified Equation (5.1).

$$
Sc_{ij} = \frac{\sum_i^3 (\mu^t_{\kappa_i} - \tau^t_{\kappa_i})}{\sum_j^3 (\sum_i^3 (\mu^t_{\kappa_i} - \tau^t_{\kappa_i}))} \tag{5.1}
$$

Step 3: Find the aggregated decision matrix $M = \left[M_{ij}\right]_{n\times m}$ by using the Equation (5.2).

$$
= \left(\begin{array}{l}
\sqrt[t]{\dfrac{\frac{\Pi_{i=1}^{n} (1-{}^{\kappa}\nu^{t}{}_{\alpha_i})^{\vartheta_i} - \Pi_{i=1}^{n} (1-{}^{\kappa}\nu^{t}{}_{\alpha_i} - {}^{\kappa}\mu^{t}{}_{\alpha_i})^{\vartheta_i}}{\Pi_{i=1}^{n} (max\{1-\nu_{\alpha_i}{}^{t}, p\})^{\vartheta_i - 1}}}{\Pi_{i=1}^{n-1} (max\{1-\nu_{\alpha_i}{}^{t}, p\})}}, \\
\sqrt[t]{1 - \dfrac{\Pi_{i=1}^{n} \frac{(1-\nu_{\alpha_i}{}^{t})^{\vartheta_i}}{(max\{1-\nu_{\alpha_i}{}^{t}, p\})^{\vartheta_i - 1}}}{\Pi_{i=1}^{n-1} (max\{1-\nu_{\alpha_i}{}^{t}, p\})}}, \\
\sqrt[t]{\dfrac{\frac{\Pi_{i=1}^{n} (1-{}^{\kappa}\nu^{t}{}_{\alpha_i})^{\vartheta_i} - \Pi_{i=1}^{n} (1-{}^{\kappa}\nu^{t}{}_{\alpha_i} - {}^{\kappa}\tau^{t}{}_{\alpha_i})^{\vartheta_i}}{\Pi_{i=1}^{n} (max\{1-\nu_{\alpha_i}{}^{t}, p\})^{\vartheta_i - 1}}}{\Pi_{i=1}^{n-1} (max\{1-\nu_{\alpha_i}{}^{t}, p\})}}
\end{array} \right) \tag{5.2}
$$

Step 4: CRITIC Method
The CRITIC approach examines the relative importance of criteria in MCDM scenarios. The calculation procedure will now be outlined in the following steps:
Step 4.1: Find the aggregated decision matrix's score value using Equation (5.3).

$$Sco_{ij} = \mu_\kappa^t - \tau_\kappa^t \tag{5.3}$$

Step 4.2: Transform the matrix Sco into standard T-SPFNs matrix by using Equation (5.4).

$$\widetilde{Sco}_{ij} = \begin{cases} \frac{Sco_{ij} - Sco_j^-}{Sco_j^+ - Sco_j^-}, & j \in \mathrm{C}_u \\ \frac{Sco_j^+ - Sco_{ij}}{Sco_j^+ - Sco_j^-}, & j \in \mathrm{C}_v \end{cases} \tag{5.4}$$

where $Sco_j^+ = \max_i Sco_{ij}, Sco_j^- = \min_i Sco_{ij}, \mathrm{C}_u$ and C_v represents the benefit-type and cost-type criteria, respectively.
Step 4.3 Calculate an estimate of the standard deviations for the criterion by using Equation (5.5).

$$\sigma_j = \sqrt{\frac{\sum_{i=1}^{n} \left(Sco_{ij} - \bar{Sco}_j\right)^2}{n}}. \tag{5.5}$$

Where $\bar{Sco}_j = \sum_{i=1}^{n} \widetilde{Sco}_{ij}/n$
Step 4.4: Equation (5.6) is used to determine the criteria' correlation coefficient.

$$r_{jt} = \frac{\sum_{i=1}^{n} \left(Sco_{ij} - \bar{Sco}_j\right)\left(Sco_{ij} - \bar{Sco}_t\right)}{\sqrt{\sum_{i=1}^{n} \left(Sco_{ij} - \bar{Sco}_j\right)^2 \left(Sco_{ij} - \bar{Sco}_t\right)^2}} \tag{5.6}$$

Step 4.5: Examine the information for each criterion by using Equation (5.7).

$$\mathrm{c_j} = \sigma \sum_{t=1}^{m} \left(1 - r_{jt}\right) \tag{5.7}$$

As $\mathrm{Cri_j}$ increases, a certain criterion has more information than others. So, the weight that is given to that criterion rises compared to other factors.
Step 4.6: Find the objective weight that each criterion should have using Equation (5.8).

$$w_j = \frac{\mathrm{c_j}}{\sum_{j=1}^{m} \mathrm{c_j}} \tag{5.8}$$

5.1. EDAS

Following the CRITIC approach, the next step involves employing the EDAS technique. This technique further refines the evaluation process. The subsequent procedure for utilizing the EDAS technique is detailed below:
Step 5: Find the average solution against each criterion by Using Equation (5.9).

$$Avg_j = \frac{\sum_{i=1}^{n} Sco_{ij}}{n} \tag{5.9}$$

Step 7: Determine the positive and negative distances from the average solution matrix, considering the benefit and cost criteria. Let C_u represent the set of benefit criteria, and C_v denote the cost criteria. Calculate the Positive Distance from Average (PDA), denoted as α, using Equation (5.10), and the Negative Distance from Average (NDA), denoted as β, using Equation (5.11).

$$\alpha_{ij} = \begin{cases} \frac{max(0, Sco_{ij} - Avg_j)}{Avg_j}, & if\, j \in \mathrm{C}_u \\ \frac{max(0, Avg_j - Sco_{ij})}{Avg_j}, & if\, j \in \mathrm{C}_v \end{cases} \tag{5.10}$$

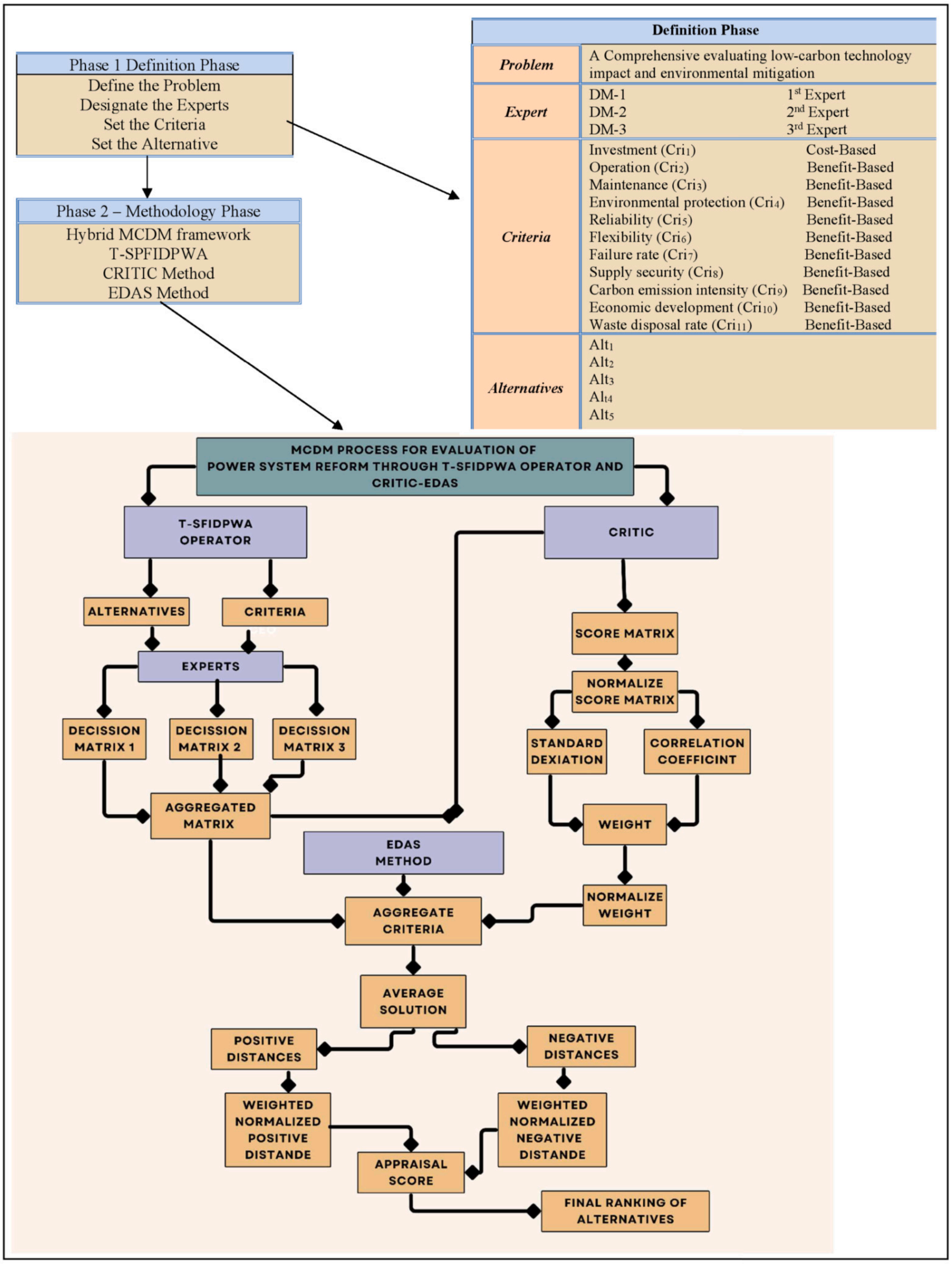

Fig. 2. Working procedure of algorithm with MCDM approach.

$$\beta_{ij} = \begin{cases} \frac{max(0, Avg_j - Sco_{ij})}{Avg_j}, & if\, j \in \mathrm{C}_u \\ \frac{max(0, Sco_{ij} - Avg_j)}{Avg_j}, & if\, j \in \mathrm{C}_v \end{cases} \tag{5.11}$$

Step 7: Use the Equations (5.12) - (5.13) to determine the weighted sum of the PDA and the NDA for each available alternative.

$$ScP_i = \sum_{j=1}^{m} \alpha_{ij} \cdot w_j \tag{5.12}$$

$$ScN_i = \sum_{j=1}^{m} \beta_{ij} \cdot w_j \tag{5.13}$$

Step 9: Normalize the values of the weighted PDA and weighted NDA by using Equations (5.14) - (5.15).

$$\mathrm{M}_i^+ = \frac{ScP_i}{\max\limits_i (ScP_i)} \tag{5.14}$$

$$\mathrm{M}_i^- = \frac{ScN_i}{\max\limits_i (ScN_i)} \tag{5.15}$$

Step 9: Calculations are made to get the appraisal score for each alternative by Using Equation (5.16). Using the appraisal score values, rank the alternatives and find the optimal solution.

$$\Lambda_i = \frac{\mathrm{M}_i^+ + \mathrm{M}_i^-}{2} \tag{5.16}$$

The algorithm is explained using a flowchart given in Fig. 2, visually illustrating its step-by-step logic and decision-making process.

5.2. Pseudo-code

Algorithm 1: Pseudocode for four techniques.

Input: Enter the number of decision-makers, let's say m

`// Each decision maker enters the decision matrix, so the number of decision matrices is m`

Input: Enter the number of alternatives (Alt) l

Input: Enter the number of criterions (cri m)

Input: Enter the value of t and p

`// This will result in the following m matrices of order` $l \times$ cri

$$DM = \begin{bmatrix} \mathrm{A}_{11} & \mathrm{A}_{12} & \cdots & \mathrm{A}_{1k} \\ \mathrm{A}_{21} & \mathrm{A}_{22} & \cdots & \mathrm{A}_{2k} \\ \cdots & \cdots & \cdots & \cdots \\ \mathrm{A}_{m1} & \mathrm{A}_{m2} & \cdots & \mathrm{A}_{Lm} \end{bmatrix}$$

$\mathrm{A}_{ij} = (\langle {}^{\aleph}\mu_{ij}^t, {}^{\aleph}\mu_{ij}^t, {}^{\aleph}\mathrm{r}_{ij}^t \rangle)$

for $i = 1$ **to** $num\_samples$ **do**
    for $j = 1$ **to** 3 **do**
        for $k = 1$ **to** k **do**
            $Sc1[j][k] = DM[i][j][k]^t - DM\_tau[i][j][k]^t$
        end
    end
end
for $i = 1$ **to** k **do**
    $score\_DM[i][1] = \mathrm{sum}(Sc1[i][:])$
end
for $i = 1$ **to** k **do**
    $Nor\_Sc[i] = score\_DM[i][1]/\mathrm{sum}(score\_DM)$
end

`// Concatenate all decision matrices by using built-in function`

$$dm = \begin{bmatrix} \mathrm{A}_{11} & \mathrm{A}_{12} & \cdots & \mathrm{A}_{1n} \\ \mathrm{A}_{21} & \mathrm{A}_{22} & \cdots & \mathrm{A}_{2n} \\ \cdots & \cdots & \cdots & \cdots \\ \mathrm{A}_{m1} & \mathrm{A}_{m2} & \cdots & \mathrm{A}_{Lcr} \end{bmatrix}$$

$\mathrm{A}_{ij} = (\langle {}^{\aleph}\mu_{ij}^t, {}^{\aleph}\mu_{ij}^t, {}^{\aleph}\mathrm{r}_{ij}^t \rangle)$

for $i = 1$ **to** 5 **do**
    for $j = 1$ **to** 11 **do**
        $prod1 = 1$
        $prod2 = 1$
        for $k = 1$ **to** 3 **do**
            $prod1 = prod1 \times \left(\frac{(1-\mathrm{dm}[i][j][k]^t)^{w[k]}}{\max((1-\mathrm{mem}[i][j][k]^t),p)^{w[k]-1}} \right)$
            if $k == 1$ *or* $k == 2$ **then**
                $prod2 = prod2 \times \max((1 - \mathrm{dm}[i][j][k]^t), p)$
            end
        end
        $\mathrm{fin\_dm}[i][j] = (1 - (prod1/prod2))^{1/t}$
    end
end

`// concatenate values to` Agg_DM

Algorithm 1: *Cont.*

```
// Apply CRITIC Method
for $i = 1$ to $L$ do
    for $j = 1$ to $cr$ do
        $s = 0$ for $k = 1$ to $m$ do
            $s = s + Agg\_DM$
        end
        $Sc_{ij} = \frac{s-p}{2*p}$
    end
end
for $i = 1$ to $L$ do
    for $j = 1$ to $cr$ do
        if j is benefit criteria then
            $\widetilde{soc}_{ij} = \frac{Sc_{ij} - \min Sc(:,j)}{\max Sc(:,j) - \min Sc(:,j)}$
        end
        else if j is cost criteria then
            $\widetilde{soc}_{ij} = \frac{\min Sc(:,j) - Sc_{ij}}{\max Sc(:,j) - \min Sc(:,j)}$
        end
    end
end
// Use built-in command std in MATLAB to find standard deviation: $\sigma_j = std(\widetilde{soc}_{ij})$
// Use built-in command corr in MATLAB to find correlation: $r_{ij} = corr(\widetilde{soc}_{ij})$
for $j = 1$ to $cr$ do
    $s = 0$ for $t = 1$ to $cr$ do
        $s = s + (1 - r_{jt})$
    end
    $c_j = \sigma_j * s$
end
for $j = 1$ to $cr$ do
    $w_j = \frac{c_j}{sum(c)}$
end
// Apply EDAS Method
for $j = 1$ to $cr$ do
    $s = 0$ for $i = 1$ to $L$ do
        $s = s + Sc_{ij}$
    end
    $Av_j = \frac{s}{5}$
end
for $i = 1$ to $L$ do
    for $j = 1$ to $cr$ do
        if j is benefit criteria then
            $\alpha_{ij} = \frac{\max(0, Sc_{ij} - Av_j)}{Av_j}$
            $\beta_{ij} = \frac{\max(0, Av_j - Sc_{ij})}{Av_j}$
        end
        else if j is cost criteria then
            $\alpha_{ij} = \frac{\max(0, Av_j - Sc_{ij})}{Av_j}$
            $\beta_{ij} = \frac{\max(0, Sc_{ij} - Av_j)}{Av_j}$
        end
    end
end
for $i = 1$ to $L$ do
    $s1 = 0,\ s2 = 0$
     for $j = 1$ to $cr$ do
        $s1 = s1 + \alpha_{ij} * w_j,\quad s2 = s2 + \beta_{ij} * w_j$
    end
     $SP_i = s1,\quad SN_i = s2$
end
// Find the appraisal Score values
for $i = 1$ to $L$ do
    $\mathfrak{N}_i^+ = \frac{SP_i}{\max SP}$
     $\mathfrak{N}_i^- = \frac{SN_i}{\max SN}$
end
for $i = 1$ to $L$ do
    $\Lambda_i = \frac{\mathfrak{N}_i^+ + \mathfrak{N}_i^-}{2}$
end
```

(a) Low-carbon strategies (b) Carbon neutrality

Fig. 3. Power systems advancements for carbon neutrality.

6. Case study

The presented case study focuses on a power company's endeavor to update its infrastructure to achieve carbon neutrality in alignment with China's ambitious carbon peak and neutrality targets [72]. The defined alternatives ($Alt_1 to Alt_5$) offer diverse strategies, including the integration of renewable energy sources, carbon capture technologies, and the retirement of coal facilities. The evaluation criteria are categorized into cost considerations (investment, operation, maintenance, and environmental protection), system performance (reliability, flexibility, failure rate, and supply security), and expected effects (carbon emission intensity, economic development, and waste disposal rate), provide a comprehensive framework for assessing the bidding proposals [73]. The research gap lies in the absence of a detailed analysis of the existing literature regarding the specific challenges, innovations, and best practices in power system transformations for carbon neutrality. A review of literature [67–71], similar to the one provided earlier, can be conducted to identify gaps in understanding the implications of different low-carbon strategies, the financial implications for power companies, and the long-term environmental and economic outcomes. Such a review would contribute to highlighting the significance of the current case study in addressing critical gaps in the existing body of knowledge and understanding the nuanced aspects of power system transformations towards carbon neutrality. Many power companies have begun to adapt and update their power systems in recent years to meet the targets of a carbon peak by 2030 and carbon neutrality by 2060, as visualized in Figs. 3a and 3b. The transition to a low-carbon economy is critical to China's carbon-neutrality policy [74]. A power company wants to update its power infrastructure to attain carbon neutrality, so it holds a public bidding process [75].

The firm expects the bidding enterprises to carry out the upgrading and transformation of the power system in a seamless and orderly manner, ultimately achieving carbon neutrality for the company's power system. Currently, five bids (Alt_1, Alt_2, Alt_3, Alt_4, Alt_5) are bidding for the power system upgrade project, including the following key ideas.

6.1. Definition of alternatives

Alt_1: Encourage the use of non-fossil energy sources and green hydrogen, as well as the conversion of coal power plants with carbon capture, utilization, and storage. Aim for zero-carbon development by promoting a circular economy in the power sector. Increase sustainability, minimize reliance on fossil fuels, and coordinate with global climate change prevention.

Alt_2: Integrate solar and wind power into the current energy infrastructure, allowing coal generation to be gradually phased out. This strategic change encourages environmentally friendly and sustainable energy practises, improving resilience and ecological sustainability in the power infrastructure. Aligns with worldwide initiatives aimed at reducing carbon emissions and combating climate change.

Alt_3: Encourage biomass blending and carbon capture technology to diversify energy sources and tap into sustainable sources for a cleaner mix. Blending biomass provides environmentally benign power, while carbon capture technology efficiently repurposes emissions, complying with global carbon neutrality targets and lowering environmental impact. These innovations demonstrate a commitment to energy sustainability.

Alt_4: Integrate CO2 collection and storage devices into the power system architecture to reduce carbon footprint and harmonize with global climate efforts. This proactive practice indicates a dedication to environmental stewardship, thereby contributing to a low-carbon energy landscape.
Alt_5: Retire coal facilities as soon as possible and increase wind and photovoltaic energy. This demonstrates a dedication to sustainable energy, which is consistent with worldwide initiatives to diversify, reduce emissions, and improve environmentally friendly electricity. Prioritizing renewables takes proactive measures towards a more environmentally friendly, sustainable energy future.

6.2. Definition of criteria

Cost:
Attaining carbon peak and neutrality necessitates considerable expenditures and financial backing for the modernization of the electricity grid. Power firms are facing rising prices due to rising labor costs and the elimination of new energy subsidies. For bidding enterprises, cost concerns that include operation, investment, environmental protection, and maintenance are critical. Comprehensive planning is required to reduce total system costs while optimizing overall effectiveness in the transformation and improvement of the power system.

1. **Investment** (Cri_1)
   The investment includes costs for research, equipment, infrastructure, development, and other essentials required for the power company's system transformation and upgrading. These expenses provide a solid foundation for later operations.
2. **Operation** (Cri_2)
   Operating costs largely include charges for procurement, manufacturing, labor, and the day-to-day operations required for the electricity system to function. To ensure the system's stability and efficiency, rational and scientific management is required for duties such as resource allocation, raw material acquisition, and product sales.
3. **Maintenance** (Cri_3)
   Maintenance expenditures include machine depreciation, maintenance, training, and leasing for maintenance staff, all of which contribute to the power company's smooth functioning. It ensures the maintenance of facilities, systems, and products throughout the whole business process.
4. **Environmental protection** (Cri_4)
   The production activities of the power firm generate a variety of waste that can harm the environment. Improper handling of industrial pollution not only damages the natural environment but also has a direct influence on human health and environmental quality. Bidding proposals should prioritize reducing environmental pollution and limiting the development of new pollutants.

System performance:
Power system augmentation and transformation invariably bring elements of randomness, volatility, and intermittency, increasing the issue of maintaining power supply and demand balance. Managing multiple system transformation strategies adds to the complexity [76]. The entire performance of the new power system is critical to achieving equilibrium and promoting extensive consumption of new energy at various times.

1. **Reliability** (Cri_5)
   Power balancing and post-accident disturbance stability are required to ensure the safe and stable operation of the power system. Failure to maintain this equilibrium risks destabilizing the electrical system, potentially resulting in outages or even the system's collapse. As a result, maintaining reliability is critical for the power system's smooth operation, allowing it to completely realize its worth and maximize benefits.
2. **Flexibility** (Cri_6)
   Addressing rising uncertainty is a big challenge for modern power systems because flexibility is a critical performance parameter. The flexible deployment and mobilization of varied resources are required to ensure the system's safe and reliable operation. This adaptability is required for the system to respond quickly to changes in supply or demand.
3. **Failure rate** (Cri_7)
   Faults and unexpected power system operating circumstances can disrupt regular operations, cause accidents, and cause damage to electrical equipment and injuries. The growing power grid, as well as advances in science and technology, place greater demands on the power system. As a result, it is critical to improve fault diagnosis and treatment to reduce failure rates and ensure power system reliability.
4. **Supply security** (Cri_8)
   As China's economy gradually recovers and energy consumption rises, certain regions confront limited electricity supplies and frequent power outages, affecting people's everyday lives and industry operations severely. As a result, modernizing the power system is critical to ensuring an overall balance of power supply and demand.

Table 4
Evaluation table given by DM 1.

DMs	Alternatives	Cri_1	Cri_2	Cri_3	Cri_4	Cri_5	Cri_6	Cri_7	Cri_8	Cri_9	Cri_{10}	Cri_{11}
DM_1	Alt_1	EE	HT	PI	ME	A	MS	HI	I	A	HT	MS
	Alt_2	I	HT	PI	I	MS	A	HI	I	HT	A	PI
	Alt_3	MS	HI	I	PI	EE	A	PI	HI	HT	MS	I
	Alt_4	A	HT	HI	A	MS	I	PI	I	ME	EE	HI
	Alt_5	PI	MS	HT	HT	ME	EE	I	HI	A	MS	ME
DM_2	Alt_1	HI	A	MS	EE	I	PI	HT	ME	A	PI	HT
	Alt_2	HT	MS	HI	PI	I	A	EE	MS	HT	I	HI
	Alt_3	PI	I	HT	MS	HI	ME	A	HI	PI	A	EE
	Alt_4	A	MS	PI	I	EE	HI	HT	ME	I	PI	A
	Alt_5	MS	EE	ME	HI	I	PI	HT	A	PI	MS	HI
DM_3	Alt_1	MS	HI	PI	A	HT	EE	I	ME	PI	MS	A
	Alt_2	HT	MS	A	HI	I	PI	HI	EE	ME	A	PI
	Alt_3	PI	HI	ME	I	HT	A	MS	PI	HT	EE	I
	Alt_4	A	I	HT	MS	PI	EE	HI	MS	PI	A	ME
	Alt_5	HI	HT	A	PI	ME	I	MS	EE	HI	PI	A

Table 5
DMs in power system reform.

Decision-Maker	Role	Key Decisions/Responsibilities	Weights of DMs
1. Government Authorities	Policymakers initiating and implementing reforms.	Decisions on market structure, privatization, regulations, and energy policy.	
$\langle 0.90, 0.20, 0.10\rangle$	$\langle 0.80, 0.15, 0.20\rangle$	$\langle 0.85, 0.20, 0.20\rangle$	0.4876
2. Regulatory Bodies	Oversee rules and bridge between government and industry.	Decide tariffs, and market rules, and ensure fair competition.	
$\langle 0.80, 0.25, 0.30\rangle$	$\langle 0.70, 0.20, 0.40\rangle$	$\langle 0.75, 0.35, 0.40\rangle$	0.2040
3. Utility Companies	Implement reforms, and adapt to new tech.	Decide on investments, technology adoption, and operational efficiency.	
$\langle 0.60, 0.40, 0.55\rangle$	$\langle 0.65, 0.35, 0.50\rangle$	$\langle 0.60, 0.40, 0.55\rangle$	0.3084

Expected effect:
Achieving the power company's upgrading and transformation goals includes assessing the potential impact of bidders' offers [77]. Given the features of the power company, the long-term benefits of the five recommendations are predicted to reveal themselves in three main areas: carbon emission intensity, economic development, and waste disposal rate.

1. **Carbon emission intensity** (Cri_9)
   The heavy reliance on old coal-fired power generation systems contributes to a rapid increase in carbon emissions in the power industry, posing a significant barrier to reaching carbon peak and neutrality. As a result, the fundamental goal of power system modernization and transformation is to minimize and reduce carbon emissions.
2. **Economic development** (Cri_{10})
   Given the significant financial support necessary for the power system, economic benefits serve as the cornerstone for the power company's long-term development. To ensure the company's long-term and healthy functioning, modernizing the power system must prioritize ensuring profitability while achieving "dual carbon" requirements.
3. **Waste disposal rate** (Cri_{11})
   The inevitable creation of additional waste during electricity generation offers a combined dilemma of resource loss and environmental pressure. Proper waste disposal becomes critical for maximizing resource utilization, putting additional demands on the new power system.

The procedure can be broken down into the following steps:
Step 1: Experts input the T-SPFNs data set with the help of linguistic terms mentioned in Table 2 for each alternative $Alt_p; (p = 1, 2, ..., m)$ under the effect of various criteria C_p as shown in Table 4.
Step 2: Determine the weights of DMs by employing the scoring function outlined in Equation (2.2). Subsequently, utilize the computed scores in Equation (5.1), and the resulting values are presented in Table 5.
Step 3: Calculate the aggregated decision matrix $M = \left[M_{ij}\right]_{n\times m}$ by using the Equation (5.2) and the outcomes are displayed in Table 6.

Table 6
Aggregated decision matrix.

Cri_i	Alt_1	Alt_2	Alt_3	Alt_4	Alt_5
Cri_1	$\langle 0.7021, 0.3186, 0.5510\rangle$	$\langle 0.8456, 0.2811, 0.4990\rangle$	$\langle 0.8000, 0.2734, 0.3856\rangle$	$\langle 0.6000, 0.3000, 0.4500\rangle$	$\langle 0.1999, 0.3636, 0.6373\rangle$
Cri_2	$\langle 0.3906, 0.3469, 0.6278\rangle$	$\langle 0.5775, 0.2957, 0.4240\rangle$	$\langle 0.2000, 0.4413, 0.7845\rangle$	$\langle 0.4149, 0.3250, 0.5519\rangle$	$\langle 0.8585, 0.2471, 0.3544\rangle$
Cri_3	$\langle 0.8000, 0.2392, 0.3281\rangle$	$\langle 0.6000, 0.3241, 0.5664\rangle$	$\langle 0.7537, 0.3146, 0.5445\rangle$	$\langle 0.8438, 0.3184, 0.5793\rangle$	$\langle 0.6208, 0.2438, 0.3502\rangle$
Cri_4	$\langle 0.6633, 0.2600, 0.3587\rangle$	$\langle 0.2000, 0.4010, 0.7129\rangle$	$\langle 0.3000, 0.3350, 0.5585\rangle$	$\langle 0.5500, 0.3412, 0.5449\rangle$	$\langle 0.8062, 0.2718, 0.4956\rangle$
Cri_5	$\langle 0.8438, 0.2644, 0.4418\rangle$	$\langle 0.3000, 0.3812, 0.6332\rangle$	$\langle 0.8761, 0.2438, 0.4531\rangle$	$\langle 0.8204, 0.0.2643, 0.3751\rangle$	$\langle 0.7500, 0.2864, 0.4572\rangle$
Cri_6	$\langle 0.8629, 0.2491, 0.3548\rangle$	$\langle 0.8000, 0.2560, 0.3786\rangle$	$\langle 0.6000, 0.2939, 0.4320\rangle$	$\langle 0.8629, 0.3113, 0.5568\rangle$	$\langle 0.6454, 0.2903, 0.5122\rangle$
Cri_7	$\langle 0.3620, 0.4078, 0.7310\rangle$	$\langle 0.5233, 0.4175, 0.7506\rangle$	$\langle 0.5500, 0.2950, 0.4206\rangle$	$\langle 0.3218, 0.3443, 0.6239\rangle$	$\langle 0.5621, 0.3556, 0.6017\rangle$
Cri_8	$\langle 0.7500, 0.3212, 0.5478\rangle$	$\langle 0.8629, 0.2907, 0.4989\rangle$	$\langle 0.8000, 0.3630, 0.6527\rangle$	$\langle 0.5500, 0.3619, 0.6050\rangle$	$\langle 0.8629, 0.3151, 0.5686\rangle$
Cri_9	$\langle 0.8000, 0.2560, 0.3786\rangle$	$\langle 0.7621, 0.1886, 0.2324\rangle$	$\langle 0.8482, 0.1365, 0.1804\rangle$	$\langle 0.8000, 0.2694, 0.4381\rangle$	$\langle 0.2000, 0.3655, 0.6429\rangle$
Cri_{10}	$\langle 0.5775, 0.2677, 0.3804\rangle$	$\langle 0.6000, 0.3242, 0.5299\rangle$	$\langle 0.8629, 0.2583, 0.3637\rangle$	$\langle 0.7240, 0.2235, 0.3294\rangle$	$\langle 0.8000, 0.2918, 0.4146\rangle$
Cri_{11}	$\langle 0.6090, 0.3120, 0.4525\rangle$	$\langle 0.8000, 0.2817, 0.5012\rangle$	$\langle 0.5335, 0.3709, 0.6581\rangle$	$\langle 0.7500, 0.3573, 0.6347\rangle$	$\langle 0.6000, 0.3330, 0.5691\rangle$

Step 4.1: Find the aggregated decision matrix's score value using Equation (5.3).

$$Sc_{ij} = \begin{array}{cc} & \begin{array}{ccccc} Alt_1 & Alt_2 & Alt_3 & Alt_4 & Alt_5 \end{array} \\ \begin{array}{c} Cri_1 \\ Cri_2 \\ Cri_3 \\ Cri_4 \\ Cri_5 \\ Cri_6 \\ Cri_7 \\ Cri_8 \\ Cri_9 \\ Cri_{10} \\ Cri_{11} \end{array} & \left[\begin{array}{ccccc} 0.2328 & 0.5052 & 0.4040 & 0.1215 & -0.0159 \\ 0.0088 & 0.1036 & -0.0363 & 0.0185 & 0.5394 \\ 0.4063 & 0.1186 & 0.3129 & 0.4966 & 0.1450 \\ 0.1890 & -0.0243 & -0.0045 & 0.0780 & 0.4170 \\ 0.5020 & -0.0130 & 0.5856 & 0.4481 & 0.3097 \\ 0.5506 & 0.4053 & 0.1221 & 0.5451 & 0.1665 \\ -0.0105 & 0.0446 & 0.0839 & -0.0033 & 0.0838 \\ 0.3058 & 0.5474 & 0.3922 & 0.0744 & 0.5446 \\ 0.4053 & 0.3361 & 0.5172 & 0.4043 & -0.0163 \\ 0.1061 & 0.1185 & 0.5501 & 0.2723 & 0.4023 \\ 0.1281 & 0.4033 & 0.0621 & 0.3001 & 0.1173 \end{array}\right] \end{array}$$

Step 4.2: Transform the matrix Sc into standard T-SPFSs matrix by using Equation (5.4).

$$\widetilde{soc}_{ij} = \begin{array}{cc} & \begin{array}{ccccc} Alt_1 & Alt_2 & Alt_3 & Alt_4 & Alt_5 \end{array} \\ \begin{array}{c} Cri_1 \\ Cri_2 \\ Cri_3 \\ Cri_4 \\ Cri_5 \\ Cri_6 \\ Cri_7 \\ Cri_8 \\ Cri_9 \\ Cri_{10} \\ Cri_{11} \end{array} & \left[\begin{array}{ccccc} 0.5228 & 0 & 0.1941 & 0.7363 & 1 \\ 0.9217 & 0.7570 & 1 & 0.9048 & 0 \\ 0.2388 & 1 & 0.4860 & 0 & 0.9302 \\ 0.5166 & 1 & 0.9552 & 0.7683 & 0 \\ 0.8603 & 0 & 1 & 0.7703 & 0.539 \\ 1 & 0.6608 & 0 & 0.9871 & 0.1034 \\ 0 & 0.5837 & 1 & 0.0761 & 0.9987 \\ 0.4892 & 1 & 0.6721 & 0 & 0.9943 \\ 0.7902 & 0.6604 & 1 & 0.7883 & 0 \\ 0 & 0.0281 & 1 & 0.3744 & 0.6673 \\ 0.1934 & 1 & 0 & 0.6976 & 0.1618 \end{array}\right] \end{array}$$

Step 4.3 Calculate an estimate of the standard deviations for the criterion by using Equation (5.5).

$$\sigma_j = \begin{bmatrix} 0.40296 & 0.41017 & 0.43262 & 0.40925 & 0.39203 & 0.47637 & 0.48229 & 0.41475 & 0.38206 & 0.42705 & 0.42054 \end{bmatrix}$$

Step 4.4: Equation (5.6) is used to determine the criteria' correlation coefficient.

$$r_{jt} = \begin{bmatrix} 1 & -0.6293 & -0.2199 & -0.8619 & 0.3085 & 0.0041 & -0.0715 & -0.2510 & -0.6520 & 0.1766 & -0.3403 \\ -0.6293 & 1 & -0.6195 & 0.8361 & 0.3393 & 0.4391 & -0.4987 & -0.5608 & 0.9894 & -0.1761 & 0.1380 \\ -0.2199 & -0.6195 & 1 & -0.1877 & -0.7226 & -0.5642 & 0.7034 & 0.9651 & -0.5819 & 0.0484 & 0.1466 \\ -0.8619 & 0.8361 & -0.1877 & 1 & -0.0974 & 0.1960 & -0.1589 & -0.2212 & 0.8484 & -0.1006 & 0.4439 \\ 0.3085 & 0.3393 & -0.7226 & -0.0974 & 1 & -0.0907 & -0.1169 & -0.5712 & 0.3902 & 0.5018 & -0.7739 \\ 0.0041 & 0.4391 & -0.5642 & 0.1960 & -0.0907 & 1 & -0.9780 & -0.6118 & 0.3056 & -0.8379 & 0.5365 \\ -0.0715 & -0.4987 & 0.7034 & -0.1589 & -0.1169 & -0.9780 & 1 & 0.7136 & -0.3754 & 0.7414 & -0.3613 \\ -0.2510 & -0.5608 & 0.9651 & -0.2212 & -0.5712 & -0.6118 & 0.7136 & 1 & -0.5129 & 0.0810 & -0.0574 \\ -0.6520 & 0.9894 & -0.5819 & 0.8484 & 0.3902 & 0.3056 & -0.3754 & -0.5129 & 1 & -0.0415 & 0.0520 \\ 0.1766 & -0.1761 & 0.0484 & -0.1006 & 0.5018 & -0.8379 & 0.7414 & 0.0810 & -0.0415 & 1 & -0.6300 \\ -0.3403 & 0.1380 & 0.1466 & 0.4439 & -0.7739 & 0.5365 & -0.3613 & -0.0574 & 0.0520 & -0.6300 & 1 \end{bmatrix}$$

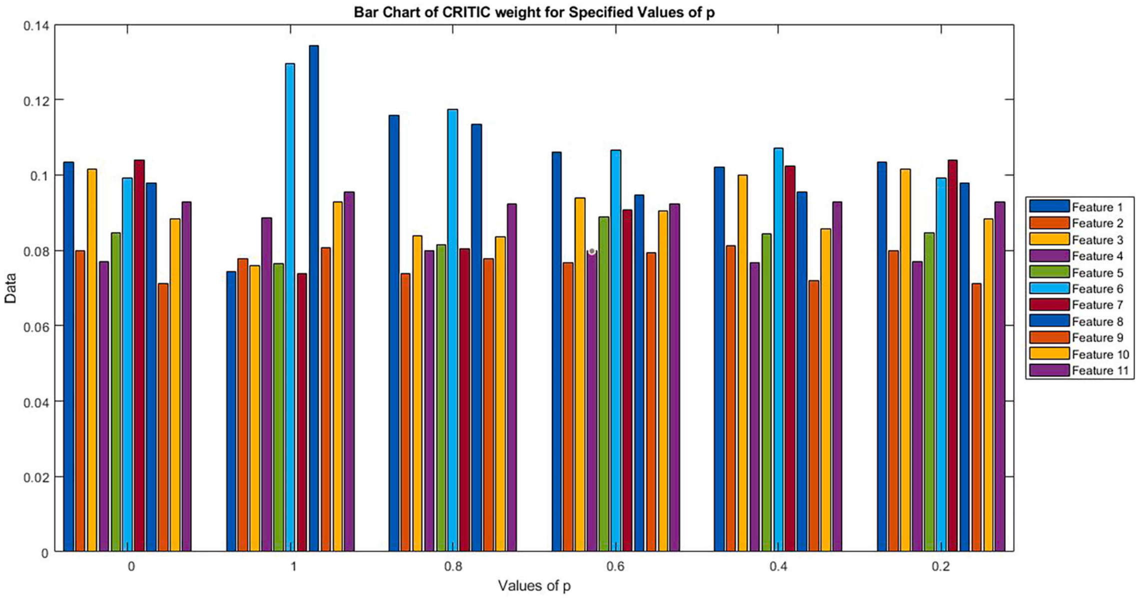

Fig. 4. CRITIC weights across p values.

Step 4.5: Examine the information for each criterion by using Equation (5.7).

$$c_j = \begin{bmatrix} 5.0517 & 3.9961 & 4.7728 & 3.8073 & 4.2468 & 5.5265 & 5.0169 & 4.5733 & 3.6593 & 4.3717 & 4.5611 \end{bmatrix}$$

Step 4.6: Find the objective weight that each criterion should have using Equation (5.8).

$$w_j = \begin{bmatrix} 0.1019 & 0.0806 & 0.0963 & 0.0768 & 0.0856 & 0.1115 & 0.1012 & 0.0922 & 0.0738 & 0.0882 & 0.0920 \end{bmatrix}$$

For different values of p, the weights of the CRITIC are depicted in Fig. 4.

6.3. EDAS

Step 5: Find the average solution against each criterion by Using Equation (5.9).

$$Av_j = \begin{bmatrix} 0.2495 & 0.1268 & 0.2959 & 0.1310 & 0.3665 & 0.3579 & 0.0397 & 0.3729 & 0.3293 & 0.2899 & 0.2022 \end{bmatrix}$$

Step 6: The positive distance from average (PDA) and the negative distance from average (NDA), represented by α and β, can be calculated by using Equations (5.10) and (5.11) respectively.

$$\alpha = \begin{bmatrix} 0.0672 & 0.9307 & 0 & 0 & 0.3698 & 0.5384 & 0 & 0 & 0.2306 & 0 & 0 \\ 0 & 0.1830 & 0.5993 & 1.1851 & 0 & 0.1324 & 0.1237 & 0.4679 & 0.0205 & 0 & 0.9948 \\ 0 & 1.2864 & 0 & 1.0343 & 0.5980 & 0 & 1.1137 & 0.0519 & 0.5705 & 0.8976 & 0 \\ 0.5130 & 0.8543 & 0 & 0.4051 & 0.2228 & 0.5229 & 0 & 0 & 0.2277 & 0 & 0.4844 \\ 1.0636 & 0 & 0.5100 & 0 & 0 & 0 & 1.1106 & 0.4607 & 0 & 0.3880 & 0 \end{bmatrix}$$

$$\beta = \begin{bmatrix} 0 & 0 & 0.3733 & 0.4425 & 0 & 0 & 1.2644 & 0.18 & 0 & 0.6340 & 0.3665 \\ 1.0246 & 0 & 0 & 0 & 1.0355 & 0 & 0 & 0 & 0 & 0.5910 & 0 \\ 0.6192 & 0 & 0.0575 & 0 & 0 & 0.6588 & 0 & 0 & 0 & 0 & 0.6929 \\ 0 & 0 & 0.6785 & 0 & 0 & 0 & 1.0835 & 0.8006 & 0 & 0.0606 & 0 \\ 0 & 3.2544 & 0 & 2.1820 & 0.1550 & 0.5349 & 0 & 0 & 1.0494 & 0 & 0.4198 \end{bmatrix}$$

Step 7: Use the Equations (5.12) and (5.13) to determine the weighted sum of the PDA and the NDA for each available alternative.

$$SP = \begin{bmatrix} 0.1906 & 0.3269 & 0.4730 & 0.2910 & 0.3465 \end{bmatrix}$$

$$SN = \begin{bmatrix} 0.3041 & 0.2452 & 0.2058 & 0.2541 & 0.6188 \end{bmatrix}$$

Step 8: Normalize the values of the weighted PDA and weighted NDA by using Equations (5.14) and (5.15).

$$\mathrm{N}_i^+ = \begin{bmatrix} 0.4028 & 0.6910 & 1 & 0.6151 & 0.7326 \end{bmatrix}$$

Table 7
The impact of the parameters p on the decision result.

Techniques	p	Alt_1	Alt_2	Alt_3	Alt_4	Alt_5	Ranking
	$p=0.1$	0.4802	0.6357	0.6856	0.5124	0.8885	$Alt_5 \succ Alt_3 \succ Alt_2 \succ Alt_4 \succ Alt_1$
	$p=0.2$	0.5248	0.6399	0.6856	0.5198	0.8899	$Alt_5 \succ Alt_3 \succ Alt_2 \succ Alt_1 \succ Alt_4$
CRITIC-EDAS	$p=0.3$	0.5208	0.6599	0.6456	0.5178	0.8890	$Alt_5 \succ Alt_2 \succ Alt_3 \succ Alt_1 \succ Alt_4$
	$p=0.4$	0.4802	0.6357	0.6456	0.5178	0.8890	$Alt_5 \succ Alt_3 \succ Alt_2 \succ Alt_4 \succ 1_4$
	$p=0.5$	0.4802	0.6357	0.6856	0.5124	0.8885	$Alt_5 \succ Alt_3 \succ Alt_2 \succ Alt_4 \succ Alt_1$
	$p=0.1$	0.2876	0.3924	0.2350	0.3579	0.3956	$Alt_5 \succ Alt_2 \succ Alt_4 \succ Alt_1 \succ Alt_3$
	$p=0.2$	0.2870	0.3912	0.2341	0.3569	0.3970	$Alt_5 \succ Alt_2 \succ Alt_4 \succ Alt_1 \succ Alt_3$
CRITIC-MAUT	$p=0.3$	0.2326	0.3924	0.2380	0.3579	0.3956	$Alt_5 \succ Alt_2 \succ Alt_4 \succ Alt_3 \succ Alt_1$
	$p=0.4$	0.2865	0.3907	0.2336	0.3561	0.3961	$Alt_5 \succ Alt_2 \succ Alt_4 \succ Alt_1 \succ Alt_3$
	$p=0.5$	0.2316	0.3714	0.2380	0.3549	0.3856	$Alt_5 \succ Alt_2 \succ Alt_4 \succ Alt_3 \succ Alt_1$
	$p=0.1$	0.4625	0.5290	0.8579	0.5339	1.0000	$Alt_5 \succ Alt_3 \succ Alt_4 \succ Alt_2 \succ Alt_1$
	$p=0.2$	0.4625	0.5292	0.8479	0.5339	1.0000	$Alt_5 \succ Alt_3 \succ Alt_4 \succ Alt_2 \succ Alt_1$
CRITIC-ARAS	$p=0.3$	0.4615	0.5480	0.7569	0.8329	0.9991	$Alt_5 \succ Alt_4 \succ Alt_3 \succ Alt_2 \succ Alt_1$
	$p=0.4$	0.5615	0.5380	0.8569	0.5319	0.9991	$Alt_5 \succ Alt_3 \succ Alt_1 \succ Alt_2 \succ 4_3$
	$p=0.5$	0.4615	0.5480	0.7569	0.8329	0.9991	$Alt_5 \succ Alt_4 \succ Alt_3 \succ Alt_2 \succ Alt_1$
	$p=0.1$	0.0501	0.0703	-0.0372	0.0831	0.0931	$Alt_5 \succ Alt_4 \succ Alt_2 \succ Alt_1 \succ Alt_3$
	$p=0.2$	0.0701	0.0603	-0.0382	0.0851	0.0961	$Alt_5 \succ Alt_4 \succ Alt_1 \succ Alt_2 \succ Alt_3$
CRITIC-MABAC	$p=0.3$	0.0761	0.0403	-0.0182	0.0651	0.0961	$Alt_5 \succ Alt_2 \succ Alt_4 \succ Alt_2 \succ Alt_3$
	$p=0.4$	0.0301	0.0203	-0.0272	0.0731	0.0931	$Alt_5 \succ Alt_4 \succ Alt_1 \succ Alt_2 \succ Alt_3$
	$p=0.5$	0.0601	0.0503	-0.0282	0.0851	0.0961	$Alt_5 \succ Alt_4 \succ Alt_1 \succ Alt_2 \succ Alt_3$

$$N_i^- = \begin{bmatrix} 0.4914 & 0.3962 & 0.3326 & 0.4107 & 1 \end{bmatrix}$$

Step 9: Calculations are made to get the appraisal score for each alternative by Using Equation (5.16). Using the appraisal score values, the ranking of the alternatives is $A_5 \succ A_3 \succ A_2 \succ A_4 \succ A_1$. The optimal alternative is A_5.

$$\Lambda = \begin{bmatrix} 0.4471 & 0.5436 & 0.6663 & 0.5129 & 0.8663 \end{bmatrix}$$

7. Sensitive analysis

We can determine the ideal solution by computing the score values for varying the parameters p and fixing the parameter $t = 0.5$ as shown in Table 7. The table provides a thorough sensitivity analysis of how changes in the parameter p affect decision outcomes. Fig. 5a demonstrates the implementation of CRITIC-EDAS, showcasing its methodology and the resulting decisions. Fig. 5b illustrates the CRITIC-MAUT method, providing insights into its decision-making process within our study. Fig. 5c presents the CRITIC-ARAS approach, highlighting its methodology and the outcomes derived from its application. Lastly, Fig. 5d depicts the utilization of the CRITIC-MABAC method, offering a visual representation of its decision-making process and the corresponding decisions made in our study. The effects of various p values on the performance of Alt_1 to Alt_5 are carefully explored for each technique. The performance rankings, which are shown in the last column, capture the relative superiority of options under various circumstances. Notably, the results show how changes in p significantly affect the decision-making environment. In addition to improving our understanding of parameter sensitivity, this comprehensive study gives decision-makers crucial insights into the unmatched robustness and adaptability built into each decision technique. This in-depth investigation not only reveals the complex interactions between various aspects but also acts as a guide for wise choice-making, enabling stakeholders to handle various situations with competence and effectiveness. Fig. 5 shows a graphical representation of the data. The graphic gives a visual overview of the dataset by illuminating significant trends and patterns. It is an effective technique for presenting complicated information clearly and understandably.

7.1. Comparative analysis

Our thorough comparative investigation carefully assessed the viability and efficacy of DM strategies within T-SPFNs. We made sure that our results were reliable and stable by emphasizing diligent analysis and incorporating thorough validation and robustness checks throughout the investigation. These factors work together to increase the importance of our research while also offering a solid basis for our findings. Table 8 provides a clear and engrossing picture of the intriguing findings of our investigation. Each inspected component helps us explore the comprehensive compared findings and gain a sophisticated grasp of the advantages and differences between various DM strategies. In essence, our study provides DMs with solid and reliable insights for the strategic integration of these T-SPFSs in addition to advancing knowledge in DM for T-SPFSs.

7.2. Discussion

The applicability of the suggested methodology to diverse real-world power system settings is a crucial factor that should be taken into account [78]. Although the study showed its effectiveness, testing the method in various situations would improve its generalizability and give a more thorough understanding of its advantages and disadvantages. The incorporation of machine learning

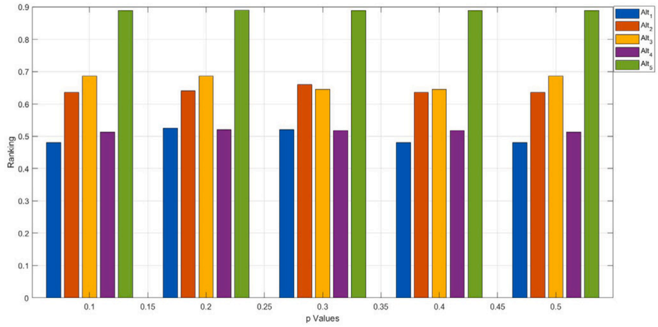

(a) CRITIC-EDAS

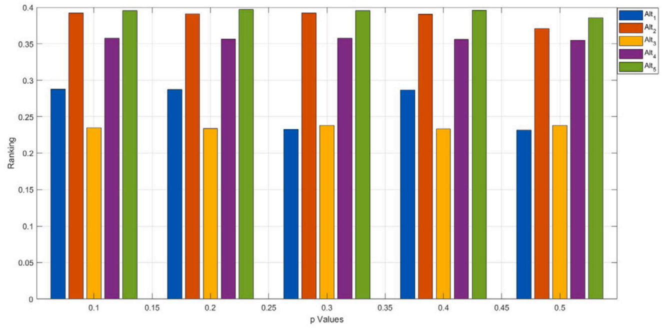

(b) CRITIC-MAUT

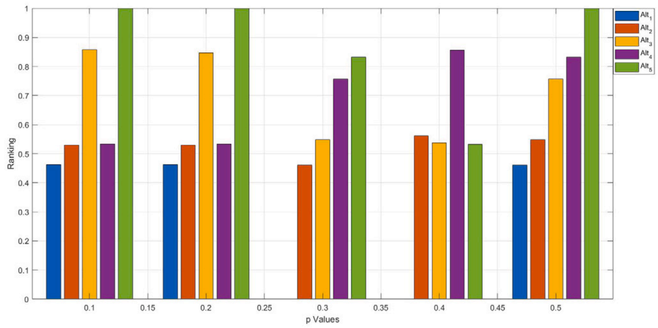

(c) CRITIC-ARAS

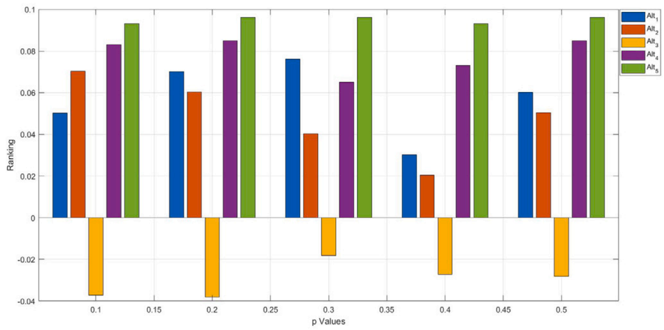

(d) CRITIC-MABAC

Fig. 5. Impact of Parameter p on Decision Results.

Table 8
Comparison of newly proposed AOs with already existing AOs when $p = .4$.

Authors	AOs	Ranking of alternatives	Optimal alternative
Mahmood et al. [83]	T-SFDPWA	$Alt_5 \succ Alt_3 \succ Alt_2 \succ Alt_1 \succ Alt_4$	Alt_5
Ullah et al. [84]	T-SPFWA	$Alt_5 \succ Alt_4 \succ Alt_2 \succ Alt_1 \succ Alt_3$	Alt_5
Khan et al. [85]	T-SPFAWA	$Alt_5 \succ Alt_4 \succ Alt_1 \succ Alt_2 \succ Alt_3$	Alt_5
Khan et al. [85]	T-SPFAWG	$Alt_5 \succ Alt_2 \succ Alt_4 \succ Alt_2 \succ Alt_3$	Alt_5
Zeng et al. [86]	T-SPFOWA	$Alt_5 \succ Alt_3 \succ Alt_2 \succ Alt_4 \succ 1_4$	Alt_5
Mahmood et al. [83]	T-SFDPWG	$Alt_5 \succ Alt_4 \succ Alt_2 \succ Alt_1 \succ Alt_3$	Alt_5
Fan et al. [88]	T-SPFAWG	$Alt_5 \succ Alt_2 \succ Alt_4 \succ Alt_3 \succ Alt_2$	Alt_5
Özdemirci et al. [89]	T-SPFAWG	$Alt_5 \succ Alt_2 \succ Alt_4 \succ Alt_2 \succ Alt_3$	Alt_5
Proposed	T-SFIDPWA	$Alt_5 \succ Alt_4 \succ Alt_2 \succ Alt_3 \succ Alt_1$	Alt_5
Proposed	T-SFIDPOWA	$Alt_5 \succ Alt_4 \succ Alt_1 \succ Alt_3 \succ Alt_2$	Alt_5
Proposed	T-SFIDPWG	$Alt_5 \succ Alt_4 \succ Alt_1 \succ Alt_2 \succ Alt_3$	Alt_5
Proposed	T-SFIDPOWG	$Alt_5 \succ Alt_4 \succ Alt_3 \succ Alt_2 \succ Alt_1$	Alt_5

methods with the suggested methodology is another fascinating topic for discussion [79]. The decision-making framework may be made more adaptable by including cutting-edge algorithms and predictive modeling, enabling it to change dynamically in response to changing circumstances [80]. An intelligent and more proactive approach to power system optimization may result from this connection.
The CRITIC-EDAS framework's sensitivity analysis has revealed how parameter variations particularly p affect the results of decisions. However, more research into how sensitive the suggested strategy is to various kinds of uncertainty would strengthen its practical application. The methodology might become more reliable and flexible if procedures are developed to deal with the uncertainties involved in power system transformation, whether they result from technological uncertainty or changing environmental conditions [81]. Given the dynamic nature of power system reform, it is important to investigate issues including shifting technology environments and legislative changes. The framework for making decisions would be more responsive to the constantly shifting situations in the power industry if these dynamic aspects were included in it [82]. Finally, doing case studies and working with industry partners could offer insightful information to bridge the gap between theoretical developments and real-world impact. The proposed technique would be put into practice and validated, which would not only demonstrate its efficacy but also make it easier for the power industry to use it in decision-making processes.

8. Conclusion

The T-spherical fuzzy interactive Dubois–Prade information aggregation approach, applied to assess the impact of low-carbon technology and environmental mitigation, offers a robust and nuanced framework. The robustness of the proposed approach is underscored by a meticulously conducted sensitivity analysis within the CRITIC-EDAS framework, illuminating the significant impact of parameter variations on decision outcomes. The superiority of the emergent T-SPF interactive Dubois–Prade procedures is evident, particularly at $p = 0.4$," as revealed through a comprehensive comparative investigation against traditional approaches. This study marks a significant leap in the field of power system optimization, offering policymakers a potent instrument to adeptly identify and rank reform efforts amidst the intricate dynamics of MCDM in the power industry. The methodological innovations not only deepen our understanding of power system reform but also empower stakeholders with sophisticated tools to navigate the challenges inherent in making strategic decisions for optimizing power system configurations.

8.1. Future work

This discovery opens up several intriguing directions for further research. First off, broadening the scope of the suggested T-SPF interactive Dubios-Prade methodology's application to a variety of real-world power system situations could yield insightful results and confirm its resilience in a range of settings. A further intriguing direction would be to investigate the incorporation of machine learning methods to improve the adaptability and prediction capacities of the decision-making framework. Its practical applicability could be improved by examining the sensitivity of the suggested approach to various kinds of uncertainty and implementing techniques to address these concerns. A more complete understanding would also result from taking into account dynamic factors of power system restructuring, such as changing technology environments and political landscapes. Last but not least, performing case studies and working with industry partners to put the suggested methodology into practice and validate it in real-world situations could close the gap between theoretical developments and real-world impact, encouraging the practical adoption of the suggested approach.

Ethical approval

Not applicable.

CRediT authorship contribution statement

Toqeer Jameel: Writing – original draft. **Muhammad Riaz:** Conceptualization. **Naveed Yaqoob:** Writing – review & editing. **Muhammad Aslam:** Supervision.

Declaration of competing interest

The authors declare the following financial interests/personal relationships which may be considered as potential competing interests: Muhammad Aslam reports financial support was provided by King Khalid University. If there are other authors, they declare that they have no known competing financial interests or personal relationships that could have appeared to influence the work reported in this paper.

Data availability

No data was used for the research described in the article.

Acknowledgements

The authors extend their appreciation to the Deanship of Scientific Research at King Khalid University, Abha 61413, Saudi Arabia for funding this work through research groups program under grant number R.G. P-2/99/44.

References

[1] Y. Duan, Y. Zhao, J. Hu, An initialization-free distributed algorithm for dynamic economic dispatch problems in microgrid: modeling, optimization and analysis, Sustain. Energy Grids Netw. 34 (2023) 1–12.

[2] M. Shang, J. Luo, The tapio decoupling principle and key strategies for changing factors of Chinese urban carbon footprint based on cloud computing, Int. J. Environ. Res. Public Health 18 (4) (2021) 1–17.

[3] J. Mo, H. Yang, Sampled value attack detection for busbar differential protection based on a negative selection immune system, J. Mod. Power Syst. Clean Energy 11 (2) (2023) 421–433.

[4] S. Xiao, Z. Wang, G. Wu, Y. Guo, G. Gao, X. Zhang, et al., The impact analysis of operational overvoltage on traction transformers for high-speed trains based on the improved capacitor network methodology, IEEE Trans. Transp. Electrif. (2023), https://doi.org/10.1109/TTE.2023.3283668.

[5] H. Wang, B. Wang, P. Luo, F. Ma, Y. Zhou, et al., State evaluation based on feature identification of measurement data: for resilient power system, CSEE J. Power Energy Syst. 8 (4) (2022) 983–992.

[6] Y. Yin, R. Zhang, Q. Su, Threat assessment of aerial targets based on improved GRA-TOPSIS method and three-way decisions, Math. Biosci. Eng. 20 (7) (2023) 13250–13266.

[7] R. Li, D. Xu, H. Tian, Y. Zhu, Multi-objective study and optimization of a solar-boosted geothermal flash cycle integrated into an innovative combined power and desalinated water production process: application of a case study, Energy 282 (2023) 128706.

[8] M.S. Chohan, S. Ashraf, K. Dong, Enhanced forecasting of Alzheimer's disease progression using higher-order circular Pythagorean fuzzy time series, Healthcraft Front. 1 (1) (2023) 44–57.

[9] A. Puška, A. Beganović, I. Stojanović, Optimizing logistics center location in Brčko district: a fuzzy approach analysis, J. Urban Dev. Manag. 2 (3) (2023) 160–171.

[10] M. Krstić, S. Tadić, Hybrid multi-criteria decision-making model for optimal selection of cold chain logistics service providers, J. Organ. Technol. Entrep. 1 (2) (2023) 77–87.

[11] N. Komazec, K. Jankovic, A systemic approach to risk management: utilizing decision support software solutions for enhanced decision-making, Acadlore Trans. Appl. Math. Stat. 1 (2) (2023) 66–76.

[12] D. Tešić, D. Božanić, Optimizing military decision-making: application of the FUCOM–EWAA–COPRAS-G MCDM model, Acadlore Trans. Appl. Math. Stat. 1 (3) (2023) 148–160.

[13] R. Choudhary, S. Ashraf, J. Anafi, Enhanced industrial control system of decision-making using spherical hesitant fuzzy soft Yager aggregation information, Acadlore Trans. Appl. Math. Stat. 1 (3) (2023) 161–180.

[14] L.A. Zadeh, Fuzzy sets, Inf. Control 8 (3) (1965) 338–353.

[15] K.T. Atanassov, S. Stoeva, Intuitionistic fuzzy sets, Fuzzy Sets Syst. 20 (1) (1986) 87–96.

[16] T. Senapati, R.R. Yager, Fermatean fuzzy weighted averaging/geometric operators and its application in multi-criteria decision-making methods, Eng. Appl. Artif. Intell. 85 (2019) 112–121.

[17] T. Senapati, R.R. Yager, Fermatean fuzzy sets, J. Ambient Intell. Humaniz. Comput. 11 (2020) 663–674.

[18] J.C.R. Alcantud, Multi-attribute group decision-making based on intuitionistic fuzzy aggregation operators defined by weighted geometric means, Granul. Comput. 8 (6) (2023) 1857–1866.6.

[19] J.C.R. Alcantud, F. Feng, R.R. Yager, An N-soft set approach to rough sets, IEEE Trans. Fuzzy Syst. 28 (11) (2019) 2996–3007.

[20] B. Cuong, Picture fuzzy sets-first results. Part 1, in: Seminar. Neuro-Fuzzy Systems with Applications, 2013.

[21] B.C. Cuong, V.H. Pham, Some fuzzy logic operators for picture fuzzy sets, in: 2015 Seventh International Conference on Knowledge and Systems Engineering (KSE), IEEE, 2015, pp. 132–137.

[22] B.C. Cuong, P.H. Thong, Two new concepts "picture fuzzy rough soft sets" and "picture fuzzy dynamic systems" in picture fuzzy systems, in: 2018 5th NAFOSTED Conference on Information and Computer Science (NICS), IEEE, 2018, pp. 87–92.

[23] M. Riaz, M.R. Hashmi, D. Pamucar, Y.M. Chu, Spherical linear Diophantine fuzzy sets with modeling uncertainties in MCDM, Comput. Model. Eng. Sci. 126 (3) (2021) 1125–1164.

[24] P.H. Phong, D.T. Hieu, R.T. Ngan, P.T. Them, Some compositions of picture fuzzy relations, in: Proceedings of the 7th National Conference on Fundamental and Applied Information Technology Research (FAIR'7), Thai Nguyen, 2014, pp. 19–20.

[25] Harish Garg, Some picture fuzzy aggregation operators and their applications to multicriteria decision-making, Arab. J. Sci. Eng. 42 (12) (2017) 5275–5290.

[26] L. Wang, H.Y. Zhang, J.Q. Wang, G.F. Wu, Picture fuzzy multi-criteria group decision-making method to hotel building energy efficiency retrofit project selection, RAIRO Oper. Res. 54 (1) (2020) 211–229.

[27] Rui Wang, Jie Wang, Hui Gao, Guiwu Wei, Methods for MADM with picture fuzzy Muirhead mean operators and their application for evaluating the financial investment risk, Symmetry 11 (1) (2018) 6.
[28] Shahzaib Ashraf, Saleem Abdullah, Tahir Mahmood, Fazal Ghani, Tariq Mahmood, Spherical fuzzy sets and their applications in multi-attribute decision making problems, J. Intell. Fuzzy Syst. 36 (2019) 2829–2844.
[29] F. Kutlu Gündoğdu, C. Kahraman, Spherical fuzzy sets and spherical fuzzy TOPSIS method, J. Intell. Fuzzy Syst. 36 (1) (2019) 337–352.
[30] T. Mahmood, K. Ullah, Q. Khan, N. Jan, An approach toward decision-making and medical diagnosis problems using the concept of spherical fuzzy sets, Neural Comput. Appl. 31 (2019) 7041–7053.
[31] Muhammad Munir, Humaira Kalsoom, Kifayat Ullah, Tahir Mahmood, Yu-Ming Chu, T-spherical fuzzy Einstein hybrid aggregation operators and their applications in multi-attribute decision making problems, Symmetry 12 (3) (2020) 365.
[32] S. Zeng, M. Munir, T. Mahmood, M. Naeem, Some T-spherical fuzzy Einstein interactive aggregation operators and their application to selection of photovoltaic cells, Math. Probl. Eng. (2020) 1–16.
[33] P. Liu, Q. Khan, T. Mahmood, N. Hassan, T-spherical fuzzy power Muirhead mean operator based on novel operational laws and their application in multi-attribute group decision making, IEEE Access 7 (2019) 22613–22632.
[34] K. Ullah, T. Mahmood, H. Garg, Evaluation of the performance of search and rescue robots using T-spherical fuzzy Hamacher aggregation operators, Int. J. Fuzzy Syst. 22 (2) (2020) 570–582.
[35] Q. Khan, J. Gwak, M. Shahzad, M.K. Alam, A novel approached based on T-spherical fuzzy Schweizer-Sklar power Heronian mean operator for evaluating water reuse applications under uncertainty, Sustainability 13 (13) (2021) 7108.
[36] M. Riaz, H.M.A. Farid, A. Razzaq, V. Simic, A new approach to sustainable logistic processes with q-rung orthopair fuzzy soft information aggregation, PeerJ Comput. Sci. 9 (2023) 1–39.
[37] I. Yaqoot, M. Riaz, A. Al-Quran, New similarity measures and TOPSIS method for multi stage decision analysis with cubic intuitionistic fuzzy information, J. Intell. Fuzzy Syst. 45 (6) (2023) 12143–12166.
[38] H.M.A. Farid, M. Riaz, q-rung orthopair fuzzy Aczel–Alsina aggregation operators with multi-criteria decision-making, Eng. Appl. Artif. Intell. 122 (2023) 1–21.
[39] H.M.A. Farid, M. Riaz, Some generalized q-rung orthopair fuzzy Einstein interactive geometric aggregation operators with improved operational laws, Int. J. Intell. Syst. 36 (12) (2021) 7239–7273.
[40] C. Jana, A. Mohamadghasemi, M. Pal, L. Martinez, An improvement to the interval type-2 fuzzy VIKOR method, Knowl.-Based Syst. 280 (2023) 111055.
[41] C. Jana, M. Dobrodolac, V. Simic, M. Pal, B. Sarkar, Ž. Stević, Evaluation of sustainable strategies for urban parcel delivery: linguistic q-rung orthopair fuzzy Choquet integral approach, Eng. Appl. Artif. Intell. 126 (2023) 106811.
[42] H.A. Alsattar, S. Qahtan, N. Mourad, A.A. Zaidan, M. Deveci, C. Jana, W. Ding, Three-way decision-based conditional probabilities by opinion scores and Bayesian rules in circular-Pythagorean fuzzy sets for developing sustainable smart living framework, Inf. Sci. 649 (2023) 119681.
[43] C. Jana, H. Garg, M. Pal, B. Sarkar, G. Wei, MABAC framework for logarithmic bipolar fuzzy multiple attribute group decision-making for supplier selection, Complex Intell. Syst. (2023) 1–16.
[44] Ž. Stević, M. Subotić, E. Softić, B. Božić, Multi-criteria decision-making model for evaluating safety of road sections, J. Intell. Manag. Decis. 1 (2) (2022) 78–87, https://doi.org/10.56578/jimd010201.
[45] M. Abid, M. Saqlain, Utilizing edge cloud computing and deep learning for enhanced risk assessment in China's international trade and investment, Int J. Knowl. Innov. Stud. 1 (1) (2023) 1–9, https://doi.org/10.56578/ijkis010101.
[46] C. Jana, M. Pal, Interval-valued picture fuzzy uncertain linguistic Dombi operators and their application in industrial fund selection, J. Ind. Intell. 1 (2) (2023) 110–124, https://doi.org/10.56578/jii010204.
[47] B.F. Yildirim, S.K. Yıldırım, Evaluating the satisfaction level of citizens in municipality services by using picture fuzzy VIKOR method: 2014-2019 period analysis, Decis. Mak. Appl. Manag. Eng. 5 (1) (2022) 50–66.
[48] M.J. Ranjan, B.P. Kumar, T.D. Bhavani, A.V. Padmavathi, V. Bakka, Probabilistic linguistic q-rung orthopair fuzzy Archimedean aggregation operators for group decision-making, Decis. Mak. Appl. Manag. Eng. 6 (2) (2023) 639–667.
[49] A. Naseem, M. Akram, K. Ullah, Z. Ali, Aczel-Alsina aggregation operators based on complex single-valued neutrosophic information and their application in decision-making problems, Decis. Mak. Adv. 1 (1) (2023) 86–114.
[50] H.A. Dağıstanlı, An integrated fuzzy MCDM and trend analysis approach for financial performance evaluation of energy companies in Borsa Istanbul sustainability index, J. Soft Comput. Decis. Anal. 1 (1) (2023) 39–49.
[51] H. Dinçer, S. Yüksel, S. Eti, Identifying the right policies for increasing the efficiency of the renewable energy transition with a novel fuzzy decision-making model, J. Soft Comput. Decis. Anal. 1 (1) (2023) 50–62.
[52] V. Pajić, M. Andrejić, M. Sternad, FMEA-QFD approach for effective risk assessment in distribution processes, J. Intell. Manag. Decis. 2 (2) (2023) 46–56, https://doi.org/10.56578/jimd020201.
[53] T.K. Paul, C. Jana, M. Pal, Enhancing multi-attribute decision making with Pythagorean fuzzy Hamacher aggregation operators, J. Ind. Intell. 1 (1) (2023) 30–54, https://doi.org/10.56578/jii010103.
[54] A.A. Khan, L. Wang, Generalized and group-generalized parameter based Fermatean fuzzy aggregation operators with application to decision-making, Int. J. Knowl. Innov. Stud. 1 (1) (2023) 10–29, https://doi.org/10.56578/ijkis010102.
[55] A.R. Mishra, P. Rani, K. Pandey, Fermatean fuzzy CRITIC-EDAS approach for the selection of sustainable third-party reverse logistics providers using improved generalized score function, J. Ambient Intell. Humaniz. Comput. (2022) 1–17.
[56] M.G. Naik, R. Kishore, S.A.M. Dehmourdi, Modeling a multi-criteria decision support system for prequalification assessment of construction contractors using CRITIC and EDAS models, Oper. Res. Eng. Sci. Theory Appl. 4 (2) (2021) 79–101.
[57] M. Akram, N. Ramzan, M. Deveci, Linguistic Pythagorean fuzzy CRITIC-EDAS method for multiple-attribute group decision analysis, Eng. Appl. Artif. Intell. 119 (2023) 105777.
[58] F. Feng, C. Zhang, M. Akram, J. Zhang, Multiple attribute decision making based on probabilistic generalized orthopair fuzzy sets, Granul. Comput. 8 (4) (2023) 863–891.
[59] M. Akram, A. Khan, A. Luqman, T. Senapati, D. Pamucar, An extended MARCOS method for MCGDM under 2-tuple linguistic q-rung picture fuzzy environment, Eng. Appl. Artif. Intell. 120 (2023) 105892.
[60] M. Akram, R. Bibi, M. Deveci, An outranking approach with 2-tuple linguistic Fermatean fuzzy sets for multi-attribute group decision-making, Eng. Appl. Artif. Intell. 121 (2023) 105992.
[61] P. Liu, P. Wang, Some q-rung orthopair fuzzy aggregation operators and their applications to multiple-attribute decision making, Int. J. Intell. Syst. 33 (2) (2018) 259–280.
[62] A. Menekse, A.V. Ertemel, H. Camgoz Akdag, A. Gorener, Additive manufacturing process selection for automotive industry using Pythagorean fuzzy CRITIC EDAS, PLoS ONE 18 (3) (2023) e0282676.
[63] S. Li, B. Wang, Research on evaluating algorithms for the service quality of wireless sensor networks based on interval-valued intuitionistic fuzzy EDAS and CRITIC methods, Math. Probl. Eng. 2020 (2020) 1–12.
[64] T. Öndeş, T. Özkan, Bütünleşik CRITIC-EDAS yaklaşımıyla covid-19 pandemisinin bilişim sektörü üzerindeki finansal performans etkisi, Gümüşhane Üniv. Sosyal Bilim. Derg. 12 (2) (2021) 506–522.
[65] H. Sun, G.W. Wei, X.D. Chen, Z.W. Mo, Extended EDAS method for multiple attribute decision making in mixture z-number environment based on CRITIC method, J. Intell. Fuzzy Syst. 43 (3) (2022) 2777–2788.

[66] N. Yalçin, E. Karakaş, Kurumsal sürdürülebilirlik performans analizinde CRITIC-EDAS yaklaşımı, Çukurova Üniv. Mühendis.-Mimar. Fak. Derg. 34 (4) (2019) 147–162.
[67] E. Brutschin, S. Pianta, M. Tavoni, K. Riahi, V. Bosetti, G. Marangoni, B.J. Van Ruijven, A multidimensional feasibility evaluation of low-carbon scenarios, Environ. Res. Lett. 16 (6) (2021) 064069.
[68] E.G. Hertwich, T. Gibon, Bouman, et al., Integrated life-cycle assessment of electricity-supply scenarios confirms global environmental benefit of low-carbon technologies, Proc. Natl. Acad. Sci. 112 (20) (2015) 6277–6282.
[69] G. Gu, W. Zhang, C. Cheng, Mitigation effects of global low carbon technology financing and its technological and economic impacts in the context of climate cooperation, J. Clean. Prod. 381 (2022) 135182.
[70] X. Liu, Y. Li, X. Chen, J. Liu, Evaluation of low carbon city pilot policy effect on carbon abatement in China: an empirical evidence based on time-varying DID model, Cities 123 (2022) 103582.
[71] X. Lyu, A. Shi, X. Wang, Research on the impact of carbon emission trading system on low-carbon technology innovation, Carbon Manag. 11 (2) (2020) 183–193.
[72] T. Xiao, Z. Lin, C. Liu, L. Liu, Q. Li, Integration of desalination and energy conversion in a thermo-osmotic system using low-grade heat: performance analysis and techno-economic evaluation, Appl. Therm. Eng. 223 (2023) 120039.
[73] B. Wu, Q. Gu, Z. Liu, J. Liu, Clustered institutional investors, shared ESG preferences and low-carbon innovation in family firm, Technol. Forecast. Soc. Change 194 (2023) 122676.
[74] Y. Yang, Z. Zhang, Y. Zhou, C. Wang, H. Zhu, Design of a simultaneous information and power transfer system based on a modulating feature of magnetron, IEEE Trans. Microw. Theory Tech. 71 (2) (2023) 907–915.
[75] M. Shirkhani, J. Tavoosi, S. Danyali, A.K. Sarvenoee, A. Abdali, A. Mohammadzadeh, C. Zhang, A review on microgrid decentralized energy/voltage control structures and methods, Energy Rep. 10 (2023) 368–380.
[76] V. Selicati, N. Cardinale, Sustainability assessment techniques and potential sustainability accreditation tools for energy-product systems modelling, J. Sustain. Energy 2 (1) (2023) 1–18.
[77] Y. Du, J.L. Wang, J.G. Lu, Optimization of magnetically coupled resonant wireless power transfer based on improved whale optimization algorithm, J. Ind. Intell. 1 (1) (2023) 63–74.
[78] S. Li, X. Zhao, W. Liang, M.T. Hossain, Z. Zhang, A fast and accurate calculation method of line breaking power flow based on Taylor expansion, Front. Energy Res. 10 (2022) 943946.
[79] S. Zhao, L. Zhang, H. An, L. Peng, H. Zhou, F. Hu, Has China's low-carbon strategy pushed forward the digital transformation of manufacturing enterprises? Evidence from the low-carbon city pilot policy, Environ. Impact Assess. Rev. 102 (2023) 107184.
[80] Y. Wang, F. Xia, Y. Wang, X. Xiao, Harmonic transfer function based single-input single-output impedance modeling of LCCHVDC systems, J. Mod. Power Syst. Clean Energy (2023), https://doi.org/10.35833/MPCE.2023.000093.
[81] Y. Wang, X. Jiang, X. Xie, X. Yang, X. Xiao, Identifying sources of subsynchronous resonance using wide-area phasor measurements, IEEE Trans. Power Deliv. 36 (5) (2021) 3242–3254.
[82] L. Lin, J. Zhang, X. Gao, J. Shi, C. Chen, N. Huang, Power fingerprint identification based on the improved VI trajectory with color encoding and transferred CBAM-ResNet, PLoS ONE 18 (2) (2023) e0281482.
[83] T. Mahmood, M.S. Warraich, Z. Ali, D. Pamucar, Generalized MULTIMOORA method and Dombi prioritized weighted aggregation operators based on T-spherical fuzzy sets and their applications, Int. J. Intell. Syst. 36 (9) (2021) 4659–4692.
[84] K. Ullah, T. Mahmood, N. Jan, Z. Ahmad, Policy decision making based on some averaging aggregation operators of t-spherical fuzzy sets; a multi-attribute decision making approach, Ann. Optim. Theory Pract. 3 (3) (2020) 69–92.
[85] M.R. Khan, K. Ullah, Q. Khan, Multi-attribute decision-making using Archimedean aggregation operator in T-spherical fuzzy environment, Rep. Mech. Eng. 4 (1) (2023) 18–38.
[86] S. Zeng, H. Garg, M. Munir, T. Mahmood, A. Hussain, A multi-attribute decision making process with immediate probabilistic interactive averaging aggregation operators of T-spherical fuzzy sets and its application in the selection of solar cells, Energies 12 (23) (2019) 4436.
[87] D. Dubois, H. Prade, New results about properties and semantics of fuzzy set-theoretic operators, in: Fuzzy Sets: Theory and Applications to Policy Analysis and Information Systems, 1980, pp. 59–75.
[88] J. Fan, D. Han, M. Wu, T-spherical fuzzy COPRAS method for multi-criteria decision-making problem, J. Intell. Fuzzy Syst. 43 (3) (2022) 2789–2801.
[89] F. Özdemirci, S. Yüksel, H. Dinçer, S. Eti, An assessment of alternative social banking systems using T-spherical fuzzy TOP-DEMATEL approach, Decis. Anal. J. 100184 (2023).